18

A Novel Directive, Dispersion-Free UWB Radiator with Superb EM-Characteristics for Multiband/Multifunction Radar Applications

D. Tran[1], N. Haider[1], P. Aubry[1], A. Szilagyi[2],
I.E. Lager[1], A. Yarovoy[1] and L.P. Ligthart[1]
[1]*International Research Centre for Telecommunication and Radar (IRCTR), Delft University of Technology*
[2]*Military Equipment and Technologies Research Agency (METRA)*
[1]*Netherlands*
[2]*Romania*

1. Introduction

The number of topside shipboard antennas doubled every decade; in 1990s they were close to 200 and have no sight of stop growing (Tavik, 2005). The over-crowded present of such many topside antennas in a limited-space of littoral warfare ship has created/caused many critical, unavoidable problem like antenna blockage, electromagnetic interference, increase RCS, worsen the effective stealthy signature of combatant ships, which is stealthy-intended designed, and most of all is the maintenance costs of multiple systems, huge numbers of repair-personnel and operators (Tibbitts & Baron, 1999). As modern warfare ships continue to require higher levels of functionality, performance and interoperability, these problems became so bad and unresolvable and gradually as severe as unacceptable. Much efforts around the globe are concurrently conducting research works on shaping their warfare sensors/systems to form network centric warfare (NCW) ready for network centric operations (NCO). As part of the NCW, combatant ships (LCS, DDX, CGX etc.) are moving towards the governing of their integrated and centralised sensor systems, in which both ITD (integrated-topside-design of radars, and electronic warfare), and TSDC (Top Side Design Communications of civil/military communications) are being seriously investigated.
The frequency occupation on board of a warship is extremely wide, from several Hz to hundreds of GHz. To reduce the topside antenna problem, with restriction to the RF sensors only, it may better to divide the occupied frequency spectrum into a number of spectra based on their related tasks. The number of spectra can be roughly divided in four main spectra: 1) VHF-UHF-L band, 2) S-band, 3) X-Ku band, and 4) K-Ka-Q band.

The ITD and TSDC conclusively assert several key demands, to name but a few:

a. Reduction of the number of topside antennas: this can be done by application active electronically scanned array (AESA) for the three last spectra previously discussed.
b. Effectively treating all the problems of topside antennas: this can be done by moving all the AESA systems to an optimized position on the desk (Tibbitts, et.al., ibid).
c. Combatting all the single-function systems: by increasing/combining the number of functions/tasks of the sensor systems, the number of topside antennas will be drastically reduced, and by doing so multi-spectrum/multifunction AESA systems will be formed.
d. Combining/integrating both ITD and TSDC as much as possible: that is collocating/grouping/aperture sharing/integrating of systems with same/close spectrum, by doing this one can reduce both space and volume and as well as the number of top-side antennas and help the NCO moves towards the governing of integrated and centralized sensor systems.
e. Choosing correct technological/functional devices/sensors with highly compact, modular, easy to install, operate, maintain, use less power, less intensive man-power for operation and services, and jointly interoperable as well. For ship-borne AESA systems, the most appropriate choice is technological tile (Lamanna & Huizing, 2006).

In the context of multiband-multifunction AESA sensor, assessments *a* to *e* all together put several stringent demands that the applied antenna must be dealed with: to be array-applicable, antenna must be 1) *unidirectional;* to prevent grating lobes the radiator must be 2) *small*, 3); to ensure stable tracking performance, preventing lost of tracking of the desired signal, reducing miss detections and false alarms, etc., the radiator must have 4) *low cross-polarization*; for accurate determination of scatter's 3D information the radiator's patterns must be: 4) *non-squint, accurate heading*; further demands are: 5) *Linear phase, negligible group delay, etc.*; to enhance resolution, smearing the multipath-lobing-dips (van Genderen, 2003), as well as supporting multiband-multifunction operation the radiator must be: 6) *wideband*; other criteria are: 7) Planar, low profiles, symmetrical pattern, etc. are crucial design issue that the radiator must comply with.

Two dominant planar antenna technologies concurrently exists, brick radiators are mostly of end-fire class, while tile radiators are plainly broadside, the choice for airborne is the first, whilst the second is favourite in littoral AESA systems. The state-of-the-art in multiband-multi-function AESA is dominant by activities in X-Ku bands. This report also focuses to technological-tile radiators and restricts to these spectra only.

Multiband-Multifunction system: perhaps the most active R&D activity in radar technology in recent years is the shift from AESA to wide-multiband-multifunction AESA radar, or sensor systems that can perform a variety of tasks/applications in different spectra within the same system. The move to active solid-state radar is possibly the only option for performing several applications with the same radar system. Numerous studies have conducted concurrently, to name but a few, for airborne systems: AN/APG-series, MP-RTIP, CAPTOR, AMSAR, Vixen-500E, Elta EL/M-2052, FSX; for ground and sea-based systems: APAR, AN/SPY-series, XBR, CVN-21, Selex, EMPAR, SAMPSON, MESAR, ATNAVICS, CEAFAR, OPS-24, MEADS, THAAD, Elta EL/M-2248, RIAS, etc. (wikipeadia, 2011)

Multiband-multifunction system requires its components must also sustain and support the functional actions that the system wants it to be executed either *sequentially* (type I) and/or *simultaneously* (type II). The problem at hand lies on how to get away from the top-side

problem and looking for as much functionalities/spectra as possible for reconfigurable/switchable/tuneable radiators either type I or II.
Based on presumable key EM-characteristics, planar radiators candidate for mutiband-multifunction AESA are roughly taxonomized in table 1.

EM-characteristics	MPA	Stacked MPA	UWBA	DUWB
Linear phase	+++	+	- -	+ + +
Phase delay	++	+	-	+ + +
Group delay	++	+	-	+ + +
UWB	- - -	-	+ + +	+ +
Flat response	+	+	- -	+ + +
Uni-directional	+ + +	+ + +	- - -	+ + +
Patterns in xoy-plane	+	-	-	+
Size	- -	- -	- -	+ +
Cost	+ +	- - -	+ + +	++
Form factor	- -	-	++	+ +

Table 1. Taxonomy of candidate radiators for UWB multiband-multifunction radar applications; The plus and minus signs roughly indicate the suitable/applicable degrees of radiator for wideband multiband-multifunction AESA applications.

Basic design considerations: Size, form factor, cost, bandwidth, gain, radiation patterns and dispersions characteristics (phase centre included) for wideband-multiband-multifunction AESA are more stringent than the short range UWB and or narrowband phase array applications. The multi-wideband-multifunction long/medium range UWB array/phased array applications (especially, when high/super fine resolution is required) place requirements on device's EM-characteristics, in particularly on a) dispersion, b) the impedance bandwidth and c) radiation patterns, and d) transmission efficiency, which is directly related to the dispersive attribute of the radiator, this will be detailed in section 6.
Dispersions is the main and most severe cause of performance deterioration in EM-devices/systems; as natural inheritabilities, it always exists in EM-devices, especially in multi-resonant structures and wideband devices. Non-dispersion is undoubtedly the most critical requirement, total elimination of dispersions from EM-devices is, however, impossible; the only possibility is partly reducing them to an acceptable limit. To realize this, the radiator must have a linear phase, has as small as possible phase delay, and possess no aberration (i.e., dispersion-free/constant group delay). Our proposed radiator advocates a unidirectional UWB radiator with extremely low transmission dispersion level, nearly dispersion-free.
Impedance bandwidth: wideband transmission capability/high-resolution relates to short pulse; to convey such pulse the necessary condition is UWB; however, a more stringent requirement is the constant characteristic of power transmission w.r.t. frequency. To fulfil this, the impedance bandwidth must be equally balance-matched over the whole interested band. The proposed directional ultra wideband (DUWB) radiator is concurrently designed so that it is not only ultra wideband but also the power are equally distributed over the possessed band, this radiator also proved that it is flexible enough in managing to have such unique property of equal-power-distribution.

Radiation characteristics: Radiators used in arrays/phased arrays must: electrically have unidirectional radiation patterns, and equally gain patterns in the array plane (XOY), and be geometrically small enough to fit in the array to prevent grating lobes, low profiles for dealing with issue related to blind angles, scan loss, etc.

Close to 60 years of development, planar microstrip patch antennas (MPA) and their variants stacked microstrip patch antennas (SMPA), and ultra-wideband antenna (UWB) have reached maturity. Numerous ground-based, space-borne, air-borne, ship-borne phased array applications are realized with these types of planar antennas with varieties of architectures.

Obviously, as previously discussed, a radiator that is suitable for multi wideband-multifunction array/phased array applications must keep the good (unidirectional pattern, linear phase of the MPA, SMPA, and ultra-wide band characteristics of the UWBA, and eliminate the bad properties of them as well. One of the challenges in the realization of wide multiband-multifunction AESA systems is the development of suitable radiators that sustain their agile wide multi-band and waveforms.

MPAs are unidirectional but they are *narrowband*. SMPAs are complicated, costly and furthermore not wideband enough. All UWBAs can not be used in planar or conformal arrays because they are mostly not compact, dispersive and their radiation's patterns are *bidirectional*. The merits and demerits of MPA, SMPA and UWBA as candidates for wideband multiband-multifunction AESA applications are generally listed in table. 1.

Directional antennas and bandwidth broadening techniques:

MPAs are inherently narrowband (<5%). Either or both increasing the substrate's height and lowering the permittivity of the dielectric slab doesn't help much, but creating other unwanted side effects such as loss in surface wave and increase cross-polarization. Application of different slot architectures (square, circular, finger, and U slot, etc.) could broaden the BW up to 50% but with the penalty of distortion in pattern symmetry and increasing of cross -polarization etc. (Lee & Luk, 2011)

SMPAs could increase the BW up to 100%, but the stacked height also increases the mutual coupling (caused by surface-wave), higher cross-polarization, higher loss, and higher thermal heat (dissipated inside the many layers), which is severe and difficult to treat in high power phased array, particularly in pulse doppler radar.

UWB antennas are inherently wideband but have not unidirectional pattern, several techniques for converting bi-directional pattern into unidirectional one are introduced such as using either earthed and floating backing/reflecting plane, cavity backed, high-impedance surface, artificial magnetic plane, quasi magnetic plane, meta-material, etc. However, by doing so the resulting radiator lost it compactness, higher profile, and the non-linearity of the associated phase, which is already a headachy problem, gets double worse due to the extraneous interference/reflection (beside its natural multiple resonances) between the top-patch and the reflecting plane underneath.

End-fire radiators (Chen & Quing, 2005) such as Vivaldi, TSA, LTSA and planar dipole are super wideband, high gain, and having directive radiation pattern ideal for airborne applications, but not for AESA applications in littoral combat systems which demands stringent requirements that end-fire radiators are not sufficient for, such as wide-scan, stable phase, low mutual coupling and stable phase centre, the last is critical for coherent radar.

UWB techniques: Investigations of all UWB directional radiators in both open and close literature, we learned: To obtain wider bandwidth, several bandwidth enhancement techniques have been studied such as: using log periodic arrays in which the different

elements are deduced from an homothetic ratio (Rahim & Gardner, 2004), introducing a capacitive coupling between the radiating element and the ground plane (Rmili & Floc'h, 2008), using microstrip-line feed and notching the ground plane (Tourette et al., 2006), using symmetrical notch in the CPW-feeding (Zhang et al., 2009), asymmetrical feeding by micro-strip line together with reduced ground plane and appropriate gap-patch distance (Karoui et al., 2010), adding T-slots for both patch and feeding strip (Rahayu et al., 2008), using cross-lot in the truncated circular patch with tapered microstrip feed line (Kshetrimayum et al., 2008). All these techniques are based on the modification of the surface current distribution to broaden the antenna's impedance bandwidth.

Unidirectional techniques: to reverse the bidirectional radiation patterns into unidirectional, several method and techniques have been introduce to design radiator(s), which are both ultra-wideband and unidirectional, by: introducing a PEC-plane under an UWB ring-slot antenna, which is matched by a balanced stub (Rao & Denini, 2006). Designing of an electromagnetic bandgap (EBG) under a ring slot radiator (Elek, et al., 2005); Using high profile foam with low dielectric constant (Suh et al.,2004); using a composite corrugated reflector under printed plannar dipole (Wu & Jin, 2010); using fractal clover leaf (FCL) as radiation patch and fed by L-probe (Tayefeh, et al.,2004); use of artificial magnetic conducting plane(AMC)(Tanyer et al,2009b).

Studying of these works, we observed that the invented radiators are i) high profile (5-66 mm), ii) using floating reflecting plane, iii) using different dielectrics in vertical stacked profiles, iv) having complicated backing topologies AMC, EBG, FCL, FSS, meta-materials, etc. These radiator are indeed UWB and unidirectional, however there are till profound issues which are not suitable for multiband-multifunction AESA applications.

We report here a compact, directional ultra-wideband antenna (DUWB) with simple grounded coplanar waveguide (CPWG) topology and special architecture which could eliminate all the unwanted effects and integrate all the merits of other candidates for multiband-multifunction AESA applications. The proposed prototype reports in this chapter belongs to the tile-class type II, it is a quasi-electric-magnetic (QEM) unidirectional planar broadside UWB antennas. The advantages of the proposed DUWB antennas with respect to other possible candidates (MPA, SMPA, UWBA) for multiband-multifunction AESA applications are roughly indicated and tabled in table 1

This chapter is organized as follow: In section 2 the definition of bandwidth is reviewed, then subsequently the concepts of quasi-electric antenna (quasi-E), quasi-magnetic antenna (quasi-M), and quasi-electric-magnetic antenna (quasi-EM) are introduced based on the basic concept of electric- and magnetic antenna. Definition and concept which is wire-version antennas that all planar antennas were derived thereof, the concepts of quasi-electric and quasi-magnetic for planar antennas are typically discussed, also definitions pertaining to qualitatively expressing the antenna's impedance bandwidth were considered. The EM-duality, Babinet's principle, Booker's impedance formula and Mushiake's relationship are discussed, which formed the main driven impetus to the design of the proposed DUWB prototype. In section 3 the topology and architecture of the DUWB antenna are described, RF-considerations on design material, PCB technology and detailed architecture and its associated parametric functions are reported. In section 4: detail works on parameter identification, investigation and optimization are discussed. As a "proof of concept", we examine the performances of the proposed radiator, and provide a methodological procedure for simplifying the multivariate optimization process, which were intensively used in previous work (Tran, et al., 2009), also parametric investigations and numerical

simulations of the proposed DUWB radiator are also reported in this section. In section 5: we report of how the implication of UWB transmission formula is simplified into the narrowband one and made it applicable to the proposed DUWB. The prototype are fabricated, tested and evaluated in both frequency- and time–domain. The measured results of reflection coefficients, co-polar and cross-polar radiation patterns are carried out and evaluated in frequency domain, whilst the transmission coefficients are measured and evaluated in time domain, the transmission's characteristics are derived and reported also section 6. Acknowledgement is expressed in section 7. Conclusions are summarized in section 8, the chapter is concluded with key references which support the arguments and assessments proliferated in this works.

2. Fundamentals and concepts

This section recapitulates and discusses the basic definitions, concepts and their corollaries, which are frequently used in this work. Section 2.1 discusses the basic definitions of impedance bandwidth, points out their defects and mistakes in usage. Section 2.2 recapitulated the concept of electric and magnetic antennas. Section 2.3 introduces the concepts of quasi electric (quasi-E) antenna, quasi-magnetic (quasi-M) antenna together with the introduction of an additional quasi-electric-magnetic concept, our proposed prototype antenna representing for this offshoot will be termed as quasi-electric-magnetic (quasi-EM) antenna. In section 2.4 the principle of EM-duality, Babinet principle together with Booker's relation and Mushiake's relationship will be wrapped-up. These fundamental principles formed the main impetuses driving to the design of the proposed quasi-EM DUWB prototype.

2.1 Bandwidth definitions

Traditional communications systems typically used signals having a percent bandwidth of less than 1%, while standard CDMA has an approximately of 2%. Early definition in the radar and communications fields considered signals with percent bandwidth of 25% or greater (measured at the *-3 dB points*) to be ultra-wideband. The recent FCC regulations (IEEE Std, 2004), which will be used as a standard throughout this text, defined UWB devices/signals as having an nominal bandwidth which exceeds 500 MHz or percent bandwidth of over 20%, measured at *-10 dB points*.

The term super wide-band (SWB) has been often used to indicate bandwidth, which is greater than a decade bandwidth. Since the percent bandwidth confused and failed to envision the SWB property adequately. The "ratio bandwidth" is exceptionally suitable and often be used for describing bandwidth of decade bandwidth or more.

There are several definitions of bandwidth circulated among our antennas and propagation society; those frequently met are octave-, decade-, fractional-, percent-, and ratio-bandwidths. The two definitions, that most frequently used, are the percent bandwidth and the ratio bandwidth. They are defined respectively as follows:

$$BW_P = 100\% \times BW \,/\, f_C \tag{1}$$

$$BW_R = BW \,/\, f_L \tag{2}$$

Where:

f_H and f_L are respectively the maximum and minimum frequency, which are mostly defined at reflection coefficient at level of -10 dB.
BW is the *nominal bandwidth* defined by $BW = f_H - f_L$
f_C is the central frequency defined by $f_C = (f_H + f_L)/2$
BW_P is the percent bandwidth and,
BW_R is the ratio bandwidth, commonly denoted as B_R = *R*-over-1, where *R* is the normalized ratio of the highest frequency to the lowest frequency defined as $R = f_H/f_L$.
Formulae in Eq.1, 2 and 3 are three common bandwidth definitions, often named as the *percent bandwidth*, the *ratio bandwidth* and the *UWB-bandwidth*, respectively.

$$BW_{UWB} = BW_P \geq \begin{cases} 25\% \ DARPA \\ 20\% \ FCC \end{cases} \tag{3}$$

The UWB bandwidth definition, which is based on the percent bandwidth, acquired the percent bandwidth with two different norms; the $BW_P \geq 25\%$ is the acquired norm defined by the defense research projects agency (DARPA) and the $BW_P \geq 20\%$ is for the federal communications commission (FCC).
The *percent bandwidth* (1) has originally been used to describe the narrow-bandwidth of conventional antennas and microwave-devices. Its usage is quite popular and often considered as a standard in many textbooks, nevertheless, it is mathematically not a solid definition because it possesses a defect when f_L approaching zero. For example, suppose that the nominal bandwidth of antennas #1 is 2GHz (0-2GHz), and antenna #2 is 20GHz (0-20GHz). It is clearly that the nominal bandwidth *BW* of the second antenna is 10 times wider than the first one; however, formula (1) indicates that both antennas have the same percent bandwidth. Another weak point is the percent bandwidth of formula (1) is always less than or equal to 200% irrespective of how wide the antenna's nominal bandwidth was. Note also that formula (1) is often mistakenly called as *fractional bandwidth*, indeed the formula (1) consolidates its meaning "fractional bandwidth" only when the factor 100% is removed.
Alternatively, the *ratio bandwidth* (2) can also be used for expressing the bandwidth of UWB or SWB antennas and devices. The defect at zero-frequency point still lurks there but the 200%-limit is lifted. The use of the ratio bandwidth is more adequate to envision the wideband characteristics of devices under investigation.
How to choose between the two formulas, although no official consent, however, the first formula (Eq.1) is often used for cases that the bandwidths are less than 100%, whilst the second (Eq.2) is for both UWB and SWB antennas/devices. It is noted that for bandwidth greater that 100%, it is better to use second formula since it reflects more correctly, especially when the impedance bandwidth of device to be investigated is super wideband.

2.2 Electric and magnetic antennas

Inspection of open and protected literature, the readers may obviously observe that planar UWB antennas, at present day, have come with a countless varieties of antennas. Almost there is a new type of antenna created for every dedicated application. These antennas vary not only in topology and architecture but also in technology and the spectra they served. It is impossible to classified or group them base on their size, shape, structure or architecture.
Planar UWB and SWB antennas which geometrically resemble its counterpart (wire)-monopole antennas are widely called monopole. However, this topological naming for the planar radiators is incorrect and confused, because the radiation pattern of all the so-called

(planar)-monopole antennas have not the shaped of the monopole but of the dipole antenna i.e., having the shape of the full-doughnut.
The term "magnetic antenna" has been occasionally employed in (IEEE STD 145, 1983) and by (Schantz & Bames, 2001) to describe antennas with radiation properties closely resembling those of a thin wire loop (Balanis, 2005). The term ”electric antenna” was also mentioned in (IEEE Std, op. cit.; Schantz et al., 2001, 2003, 2004; and Baum, 2005). Formal definition, however, is still lacked. To keep this chapter self-content and avoid cross-reference, and to avoid ambiguities, formal definitions for planar antennas are summarized and given hereafter:
As a first step, let the *base plane B*, be the plane comprises the antenna's effective radiating/ receiving aperture, and let *n* be the unit normal vector to this plane, with reference to Fig.3, *B* can be assimilated into *xOy*, while $\mathbf{n} = \mathbf{i}_z$.
Assume that the field has a transverse electromagnetic (TEM) distribution propagating along the base plane. Then the following cases can be distinguished:

- The case when the base plane *magnetic field* $\mathbf{H}(\mathbf{r})$, with $\mathbf{r} \in B$, is directed along n, the radiator is referred as *magnetic antenna*.
- In the case when the base plane *electric field* $\mathbf{E}(\mathbf{r})$, with $\mathbf{r} \in B$, is directed along $\mathbf{n}$,the radiator is referred as *electric antenna*.
- *Corollary*: If there exists a structure which sustains both $\mathbf{E}(\mathbf{r})$ and $\mathbf{H}(\mathbf{r})$, with $\mathbf{r} \in B$, is directed along $\mathbf{n}$, then the radiator is referred as electric-magnetic antenna.

The above definitions are strictly applied to structures that support propagating-and-non-rezo TEM- field distributions only, so that the waveguide case is automatically excluded by this TEM regard. We note here that the above definition have not taken in to account the diffraction effects at the edges/vertexes/corners of the metallic/dielectric material that constituent the transmitting/receiving aperture.

2.3 Quasi-electric, quasi-magnetic and quasi-electric-magnetic antenna

Quasi-E and Quasi-M antennas: In general, as discussed in previous section, planar antennas can either be assimilated into the class of electric antenna or magnetic antenna. However, most of the cases, particularly in planar antenna configuration, the topology of the radiating apertures may prevent the above-indicated conditions from being rigorously satisfied. Even in such cases, either one or the other of the two situations may prevail, thus correctly determine the type of the antenna. For instant, a radiator for which the magnetic field strength $\mathbf{H}(\mathrm{r})$ or the electric field strength $\mathbf{E}(\mathrm{r})$ is parallel to $\mathbf{n}$ over most of the effective aperture will be denoted as quasi-magnetic antenna, or quasi-electric antenna, respectively.
Obviously, planar antennas fed by microstrip-line or co-planar-waveguide can be classified as quasi-electric or quasi-magnetic antennas, respectively. For example, the RAD-NAV antenna (Tran, et al., 2010) and (Tran, et al., 2007) are quasi-E and quasi-M antenna, respectively.
E-M antenna and Quasi E-M antenna: Now that if there exists antenna which simultaneously support and has both electric and magnetic field perpendicular to the base plane *B*, **r**egarding to the concept outlined in the section 2.2, such an antenna should corollary be *EM-antenna*.
In practice, there could have antenna that itself possesses topology and architecture that only partially gratifies both of conditions asserted in section 2.2, obviously such antenna

should be classified as *quasi-EM antenna*. As will be demonstrated hereby, our proposed prototype falls in the class of quasi-electric magnetic (quasi-EM) antenna.

2.4 Babinet's principle, Booker's formular and Mushiake's relationship

Babinet principle can be used to find complementary impedances (Mushiake, 1996). Babinet's principle states geometrical-optically that when a field behind an infinite screen with an transparent opening is added to the field of a opaque complementary structure, then the sum is equal to the field where there is no screen. Rigorous proof can be found in standard optics or antenna textbooks (Hecht, 2001; Balanis 2005; Stutzman & Thiel, 1997).
Booker extended the Babinet principle to vector electromagnetic fields, with polarization taken into account and derived a useful formula of practical interest for antenna engineers and designers.

$$Z_s Z_d = Z_0^2 / 4 \tag{4}$$

Where,

- Z_s is impedance of the slot antenna, the magnetic impedance.
- Z_d is the impedance of the electric antenna, i.e the complementary antenna of the corresponding magnetic antenna.
- $Z_0 = 120\pi$ Ohm is the free-space impedance.

Mushiake investigated Booker's formula relation and applied to a class of Self-Complementary Antennas, and found that the antenna's optimum impedance bandwidth is determined by (Mushiake, 1996)

$$Z_{\text{in}} = Z_0 / 2 \approx 60\pi\Omega \approx 180\Omega \tag{5}$$

Where Z_d and Z_S are input impedances of the metal part (electric source) and slot radiating part (magnetic source), and Z_0 is the intrinsic impedance of the media in which the structure is immersed. In practice, Z_s is not only the impedance of the slot, but can be viewed as the complementary impedance (a dipole or loop). A more general definition of intrinsic impedance $Z_0 = \sqrt{(\mu / \varepsilon)}$.
A strip dipole and a slot can be considered as complementary radiators. Booker had shown (Booker, 1946), that the electromagnetic fields of a slot and its complementary dipole are identical excepts that the vibration directions of the electric and magnetic field are interchanged. Both impedance and patterns can be found in the same manner in accordance with the duality property of Maxwell's equation (i.e., interchange E with H, H with -E, ε with μ, and μ with ε)

3. Antenna topology and architecture

The conceptual idea: starts form the Booker's impedance relation between the complementary sources. The starting point in the design of the antenna advocated in this work is the logical selection of the correct topology that could possibly support the requirements discussed in previous section. The topology of the proposed radiator is depicted in Fig.1a. The developed radiator anticipated several advantages of grounded coplanar waveguide (CPWG) topology to create an antenna structure which is capable of either supporting both quasi-E and quasi-M to form a quasi-EM antenna.

3.1 Antenna topology

Topological choice: investigation of Booker's formula and Mushisake's relation, we anticipated that impedance bandwidth of the antenna can be improved by creating a structural topology, which possesses design parameter(s) which can be used to balance the impedances of both of its electric-part and magnetic part. To have that, one has to create or take a topology that inherently posses both electric and magnetic part in the same structure i.e. creating a quasi-EM antenna.

The CPWG is quite suitable for that purpose, as seen in Fig.1, the internal copper part of the CPWG's upper-side-ground can be etched away to form a closed a loop this will function as the magnetic loop antenna (which is *current-driven* by the current along the edge of the loop), while the central signal line is protruded further into the loop to form the electric antenna (which is *voltage-driven* by the applied potential between the stub and the lower ground plane).

The stub is expanded in width and length to form a patch as show in Fig.2. The patch's width and length will be chosen to match the Mushiake's impedance value, as will be detailed in the next section. The CPWG under ground plane form a grounded reflecting plane to make the radiator unidirectional. Another distinct feature of CPWG is that it inherently possesses a mechanism for to prevent mutual coupling, because there is artificial electric conducting plane (AEC) at the edge of the radiator since both ground planes (under and upper) have the same grounded potential when the SMA is connected.

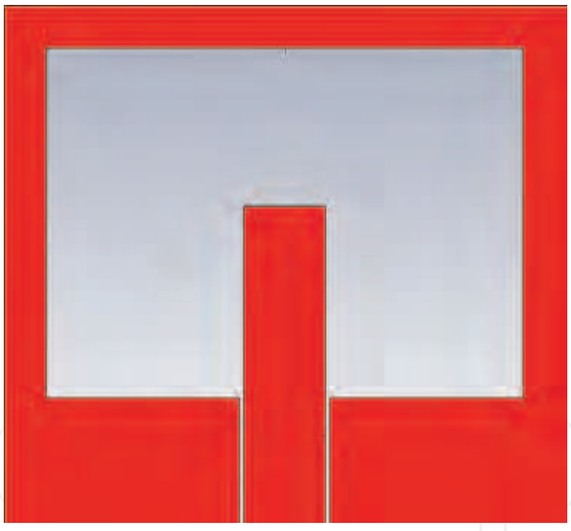

Fig. 1. CPWG topology comprises both electric-source and magnetic-source.

3.2 Antenna architecture

The starting point in the design of the SWB antenna reports in this section is mainly credited to the original radiator (Tran et al.,2009), whose topology is planar, as sketched in Fig.2, with structural topology comprised of following stack-ups:

- Single dielectric layer to provide structural rigidity.
- CPWG topology is chosen as single feeding structure which supports both electric and magnetic radiating part.
- The quasi-M radiating section is formed by etching a slot as show in Fig.1.

- The quasi-E radiating section is formed by modifying the stub (Fig.1) to form a patch as show in Fig.2, The antenna patch is directly connected to the CPW-feeding, together with the ring both magnetic and electric radiating part form a single planar pattern run on top of the structure.

The CPW feeding structure has been chosen because of it well-behaved properties: such as negligible radiation, low loss, the effective dielectric is constant over a sustained wide frequency range, where the later property is more suitable for super-wide-band feeding a SWB-radiator than the micro-strip line (Simons, 2001).

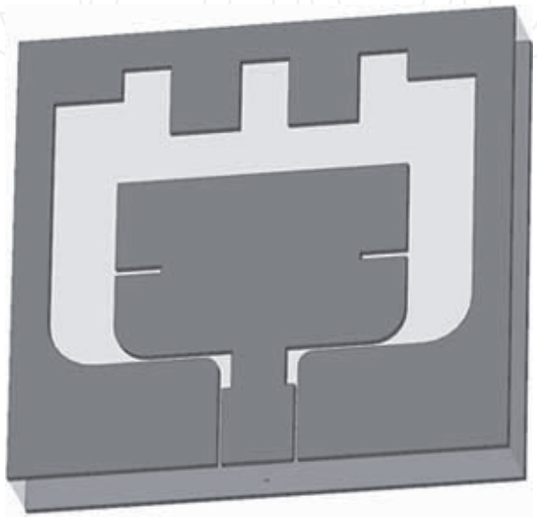

Fig. 2. The proposed architecture based on CPWG Topology

As discussed in pervious section, we strived to create an architecture such that the radiator comprises of both electric and its complementary part to improve the impedance bandwidth. The architecture of Fig.2 advocates the following features: compactness, simplicity, unidirectional, low-dispersion, and ultra-wideband.

Compactness: The antenna is designed in such a way that its outer dimension must comply with the AESA dimensional constraint requirement on grating lobe up to certain degree of steering angle.

Unidirectional radiator: the CPWG topology itself has the base (under) ground plane, this automatically supports and functions as grounded reflecting plane for both of the quasi-electric source (the stub/patch) and quasi-magnetic source (slot inside the ring).

Dispersion control: the right side of Booker's equality (Eq.4) is real, this implies that when perfect complementary takes place the inherent reactance and susceptance (in the left-side of Eq.4) of the quasi-EM radiator must be vanished. This can only be satisfied (up to some degrees of satisfaction) if we could created some parameters to control the current flows on the quasi-E radiator and the slot area of the quasi-M counterpart.

Ultra-wideband: by appropriate balancing the impedances of electric and magnetic part in accordance with the Mushiake's optimum values (Eq.5), wideband matching is feasible.

The proposed radiator's architecture, which is based on the CPWG topology (Fig.1), is shown in Fig.2. Perfect electric conductors (PEC) are situated on both side of the electric slab, the underneath PEC functions as ground plane, while the upper ring side serves two functions both ground and matching. With the different stubs that are visible in Fig.2 being

electrically connected to the waveguide's grounded ring, the employed top centre-signal stubs are extruded down to control (enhance) the current flows along the quasi-E patch antenna, this makes the quasi-E radiator electromagnetic-virtually longer in length, which effectuates the resonance and shifts it to lower frequency.
The structure is kept small for allowing for susceptance matching in the higher segment of the operational frequency band. The notches in the patch physically and electromagnetically force the currents to flow along longer paths, making the patch (virtually) extra longer; this makes it possible to neutralize the reactance in the lower end of the frequency bandwidth. The stubs at the upper-side of the ring are extruded down to form capacitive gaps that provide paths for the flow of the displacement currents. In this manner, more degrees of freedom are created for tuning the antenna at lower frequencies. To manage the match between the patch and feeding section, the carves at the feeding point (the 'neck') of the patch allow a smooth transiston from CPWG to both of the patch and the loop. More details on the design and working principles of this radiator can be found in the original article which discussed the first version of the quasi-EM antenna (Tran et al., 2010)

3.3 Design and material consideration

The propose prototype with topology and architecture depicted in fig.1 and 2. with design dimensions listed in table.1, have been fabricated on Duroid RT 5880 high frequency laminate with substrate height h=5.375 mm, copper cladding thickness t=17μm, relative dielectric constant εr=2.2, electric and magnetic loss tangents are given by tan δ_E=0.0009 and tan δ_H=0, respectively. The foremost reason of choosing this material is that it could relatively afford SWB frequency range up to 77 GHz (Huang et al., 2008, p.64). Other reasons are assessments related to temperature, moisture, corrosion, stability and missile-proof applications, which were investigated in details and reported by (Brown et al., 1980).

3.4 Antenna design parameters

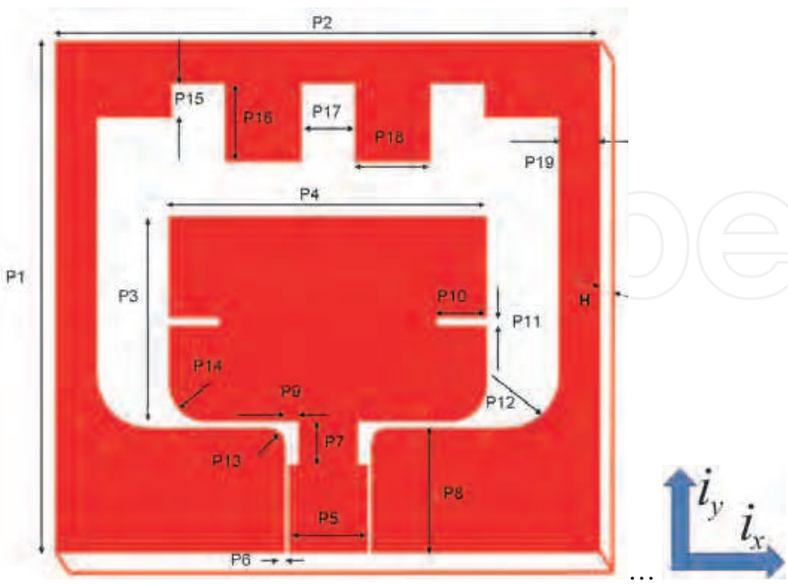

Fig. 3. The quasi-electric-magnetic antenna: design parameters.

All the cryptic design parameters are shown in Fig.3, Their dimensions (in mm) and their design-functionalities are listed together in table 2.

The antenna is designed to cover both of the X & Ku bands, emphasized on wideband multispectrum-multifunction AESA X-band applications (8-12GHz) and satellite communication (10.95-14.5GHz). The central frequency is taken at centre of the X-band f_C =10 GHz, the maximal dimension is limited to $d_{max} < (1+\sin\theta)^{-1}$, where θ is 60^0, the scanned angle required.

In order to accelerate the optimization process, several parameters are kept fixed, as well as empirically chosen as follows:

a. Antenna-boundary constraint parameters: square radiator is chosen in accordance with technological-tile applied to phased array with dense grid. The nominal values are P1 = P2 = 13.4 mm which is 0.45 λ_C and 0.54 λ_H at 10GHz and 12GHz, respectively.
b. Feeding parameters: the topology of the feeding structure is CWPG, where the interdependent parameters signal width P5 and gap P6 are chosen such that the feeding line is 50 Ω, their nominal dimension are given in table 2. Note: use has been made of the CPWG-feeding-parameters, this interdependent parameter pair (P5, P6) provides a flexibility for controlling the separation of oscillation positions at the transition between the feed and the patch, note that the two oscillation points are chosen wide enough to dispread the currents flow on the electric-patch and are attracted by the two inner stubs on the upper side of the ring.

Par	**Dim.**	Description	Define/ Create/ Control
P1	13.4	ant. length	Fund. resonance / modif
P2	13.4	ant. Width	Shifting/moving the resonance
P3	4.95	patch length	Shifting/matching the resonance
P4	7.81	patch width	Matching/balancing the resonance
P5	1.94	sig. width	Impedance paired with P6
P6	.102	gap width	Fixed, Impedance paired with P5
P7	.9	carve length	Transformer length
P8	3	feed length	n.a.
P9	.25	carve depth	Transformer match
P10	1.86	notch length	Shifting BW
P11	.21	notch width	Match BW L/R
P12	1	slot mitered	Field matching / shaping
P13	.5	CPWG mitered	Imp. transform / match
P14	1	stub mitered	field matching / shaping
P15	.84	stub length	Ind. tuning /match
P16	1.9	stub length	Cap. tuning /match
P17	1.33	Separation	Adjusting /shifting resonace
P18	1.86	stub width	Cap./ Ind. balance
P19	1	ring width	Mutual coupling
H	5.537	Substrate height	RT5880, ε_r=2.2; tanδ=0.0009, cladding ½ oz

Table 2. Design parameters (in mm) and their functions

c. The ring width P19 plays an important role in preventing coupling effect causes by lateral wave and space wave, in general the wider the ring the lower (i.e better) the mutual coupling. However, we are limited by the size constraint in scanned array (as discussed in a), also we can not extend the width of the ring inwards because that will decrease the magnetic area and disturb the balance between the electric and magnetic impedance balance. 1mm is the widest we are tolerated to have in this design.
d. The carving parameter P9 add an extra parameter mechanism for fine tuning the mating between the feeding line to the electric patch, the boundary for this parameter is from 0 to 0.25% of P5's nominal value.
e. Blending edge parameters P12 & P14: these have negligible on impedance bandwidth but smoothing them will prevent the cross-polarization due to the diffraction of the two perpendicular edges both on the ring and the patch, we took an empirical value of 1mm.
f. The fixed inner width of the slot (P2 - 2xP19), on this upper ring we place four stubs with equally width P18, their inter distance is balanced by same distance P17.
g. Outer stubs are implemented to control the area of the quasi-M radiator, whilst the two inner-stubs are for controlling the electrical length of the quasi-E radiator. The idea of introducing the outer stubs with protruding parameter P15 on the top corners of the ring are not only for balanced matching the impedance of the quasi-E (patch) to that of the quasi-M (slot), but "also" for controlling the radiation patterns of the slot.
h. Patch: the patch is a rectangular patch with under-corners blended (see *e*), the patch width P4 and length P3 will determine the resonances of the quasi-E radiator, in order to shift the resonance to the lower frequency region (and also keeping the balance between the E and the M-radiator) the two inner stubs are extruded downward to provide a GND potential close to the top of the patch which attracts the currents on flowing upward instead of sideward, this virtual extends as of the patch is electromagnetically longer. The two side notches of the patch are introduced to push the current flows more parallel along the resonance length of the electric radiator.

Optimized values are listed in table 2, all the dimension are in mm, also short description of their functions are included in the same table. Since the proposed radiator comprised of two quasi actuators (E,M), which share the same compact structure all the parameters influence both of the radiators, however depending on their position their influences will be predominant to E or M radiators.

4. Parameter identification, investigation and optimization

With the many design parameters possessed by our proposed prototype, global multivariate-optimization is possibly impossible. In dealing with structure with such many parameters, all the design parameters of the proposed architecture, each indeed has different influential magnitude on certain aspects of the radiator's overall performance. *Optimization*: in dealing with the many parameters as this architecture exhibited, We strived to reduce them by singling out the critical design parameters, by closely inspection of the parameters, they can be gratified into two groups based on their main functional-effect, that are resonance-matching parameters and resonance-shifting parameters

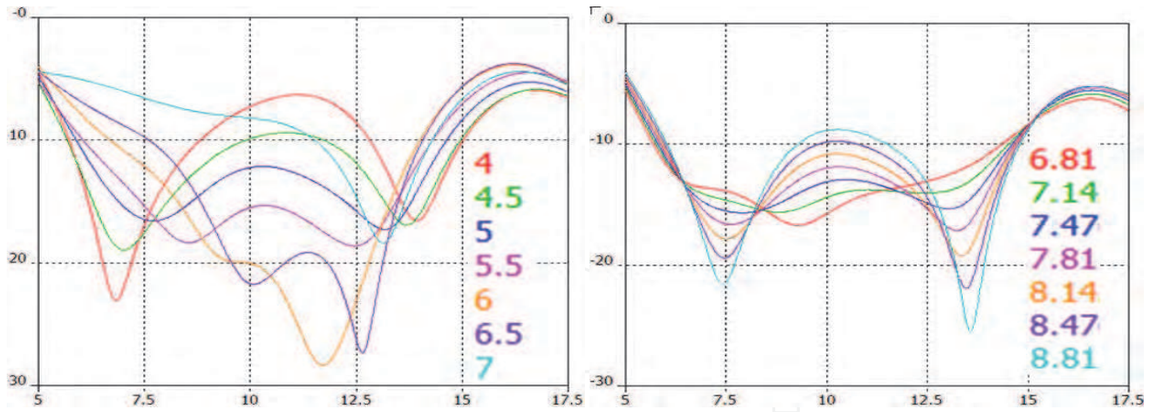

Fig. 4. Parametric investigation: a) effects of the path length P3; b) effects of the patch width P4

The microstrip patch antenna inside the slot, functionally acts as an embedded quasi-E antenna. Conventional design rules for MPA is exploited and used as start values for both parameter sweeping and optimization process. As usual the length P3 of the patch set the resonance frequency (the longer the patch the lower the resonance frequency), It is noted that the length of the patch is extended by the inner stubs, this effects is used to control/create the lower resonance, these effects are plotted in Fig.4a. The patch width P4 provide the balance-match the impedance bandwidth, the effect of P4 is clearly seen in Fig.4b. Since the right hand side of the Babinet-Booker impedance relation is a constant, and a optimum value of 180 Ohm was found by Mushiake (Eq.5), we need to control only one impedance (either electric or magnetic part), the other will result automatically. Since Z_D can be decreased by increasing the width P4 of the patch, this is acceptable as far as the ratio of P4/P3 does not exceed 2.

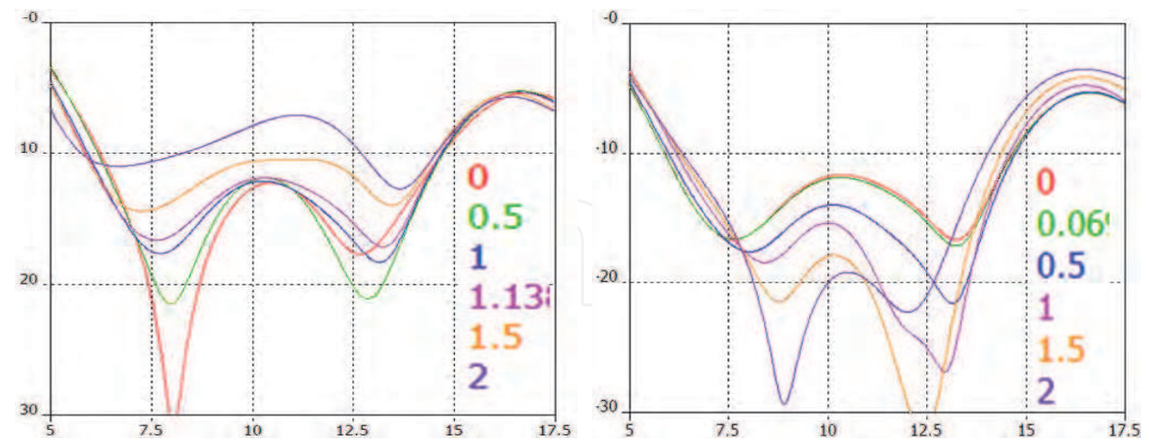

Fig. 5. Parametric investigation: a) effects of the inner-stub P16; b) effects of the outer-stub P15

In our architecture, we are not allowed to vary the width P4 freely because that will disturb the impedance balance between the magnetic and the electric parts, the only way to set the resonance is, first, to sweep the length parameter P3, we see that in contrast with traditional design, the length (instead of the width) is used to set the resonances, the low-resonance is

controlled by shortening the length P3, whilst high-resonance is by lengthening it (as shown in Fig.4a). The impedance bandwidth is balanced by limitedly sweeping the width parameter P4, we saw that P4 has no shifting-function on both low and high resonances but only just balancing them.

Fig.5a and 5b showed the effects of virtually varying the electrical length of the quasi-E, and the magnetic-area of the quasi-M by varying the two inner-stubs P16 and outer-stubs P15, respectively. The electric-effects of the inner stubs P16 are anticipated to control the low resonance (Fig.5a) while the magnetic-effects of the outer stubs P17 are for the higher resonance (Fig.5b). P16 and P15 demonstrated strong influences both on matching the resonances and balancing them as well but with marginal shifting-functionality.

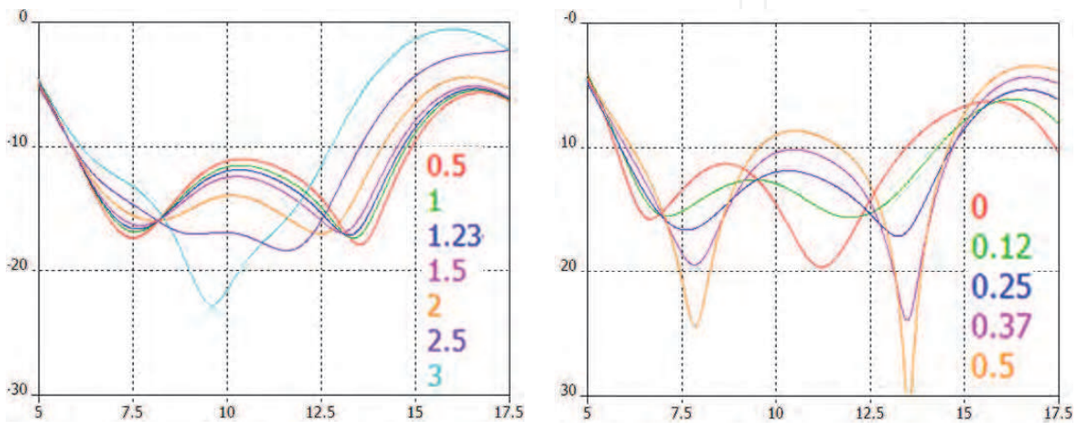

Fig. 6. Parametric investigation: a) effects of the notch length P10; b) effects of the carving P9.

The notch length P10 is another parameter which can be used to control the electrical path length of the quasi-E radiator, and to pull down the hump at mid-band, balancing the resonance, and widening/narrowing the bandwidth as clearly shown in Fig.6a. The carving parameter P9 can be utilized to enhance the resonance matching, to widen the bandwidth, the effectuated usages of this parameter is not totally exploited but clearly displayed in Fig.6b. Note that this parameter also demonstrated its potential of creating multiband radiator, which can be seen by closely inspection of Fig.6b.

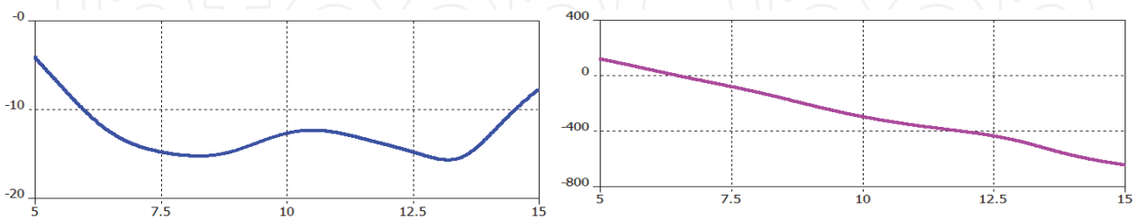

Fig. 7. a) balanced reflection coefficient; b) perfect linear phase of reflection spectrum

Fig.7a shows the reflection coefficient (S11). It is optimized such that all strong and deep resonances are merged or faded out, in this manner, as a result, we have

- Obtained a unidirectional-radiator with the widest impedance bandwidth ever recorded on a single substrate layer (over 100% percent BW), as shown in Fig.7a.

- Obtained an equally-flat power delivery to the radiator in the dedicated band.
- Achieved a nearly perfect linear phase, Fig.7 b demonstrated an excellent linear phase which covers the whole designated X to Ku bandwidth
- Limited the dispersive of the group delay to the lowest level ever designed (Fig.8a), this figure displayed a smooth and negligible group delay of sub-nanosecond level as shown in the plot with magnified scale of Fig.8b.
- The X-band transmission efficiency of the radiator is over 94%, with constant, flat power-delivery and low inband-deviation of only 0.1dB (Fig. 9).

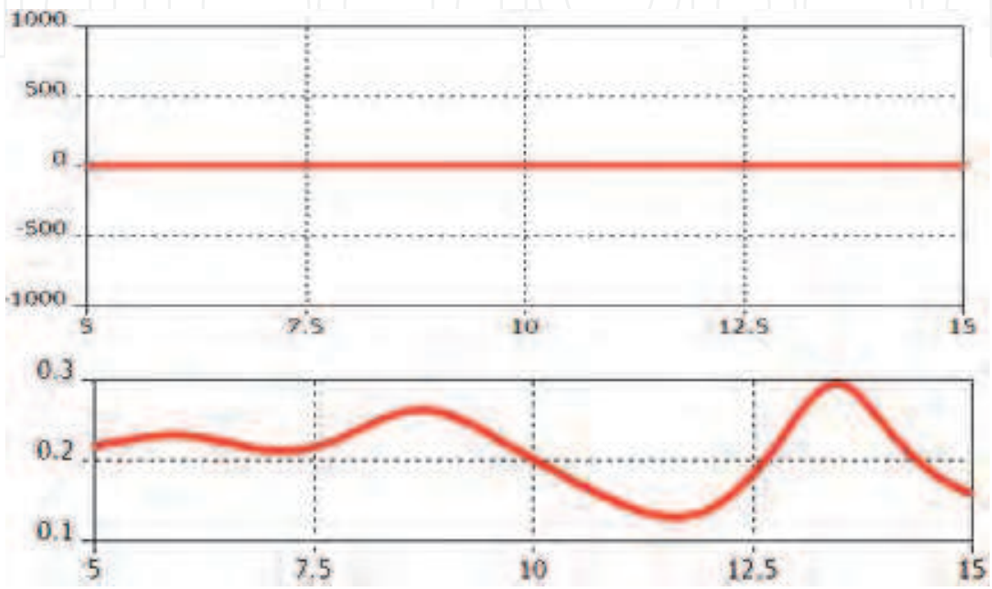

Fig. 8. a) Perfect group delay, b) magnification in sub-nanosecond scale

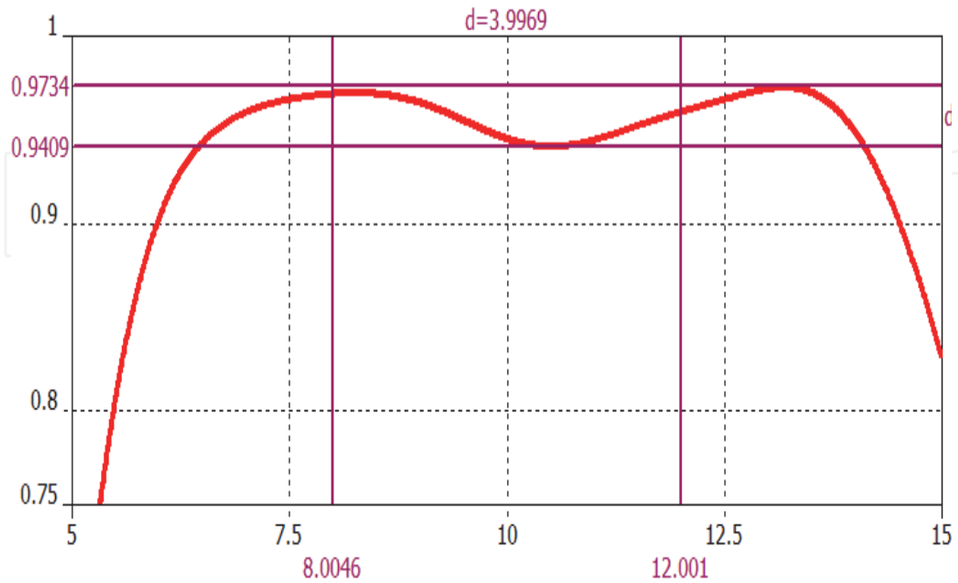

Fig. 9. Constant and high transmission power effciency; inband-deviation only 0.1dB

5. Transmission efficiency

In system point of view, regardless of narrowband or ultra-wideband, the antenna's transmission efficiency η_{TRAN} is the *most* vital parameter for gauging the effectiveness of the radiator (Wu et al., 2003). Taking the *transmitting mode* as investigation case (the *receiving mode* is equally valid by reciprocity theorem).

$$\eta_{trans,NB} = 1 - |S_{11}|^2 \tag{6}$$

$$\eta_{trans,UBW} = \frac{\int_0^\infty P_{in}(f)(1-|S_{11}(f)|^2)\,df}{\int_0^\infty P_{in}(f)\,df} \tag{7}$$

For narrowband Eq.6 is the standard norm for gratifying the performance of the applied radiators/devices/systems. This equation is valid by assuming that $|S_{11}|$ is constant over the designed signal bandwidth, and as was discussed and shown in table.1, MSAs have all criteria for the equation to be applied. For UWBAs however, the return loss $|S_{11}(f)|$ is naturally a function of frequency, for accurate determination of the transmission efficiency, one have to integrate over the frequency band to account for all the dispersion variation in the designed band in accordance with Eq. 7.

The proposed DUWB radiator is ultra-wideband, however, because its return-loss $|S_{11}|$ is nearly constant over the designated band, as discussed in previous section, without loss of generation the term $(1-|S_{11}|^2)$ can be take out of the integration sign, and as a result the UWB transmission efficiency formula (Eq.7) is reduced to narrowband one (Eq.6); In other words the narrowband transmission efficiency equation (Eq.6) is exceptionally applicable to our proposed radiator despites the contrary fact that our proposed radiator is an UWB radiator. the transmission efficiency of the proposed DUWB radiator is calculated and shown in Fig.9.

6. Physical implementation of the prototype

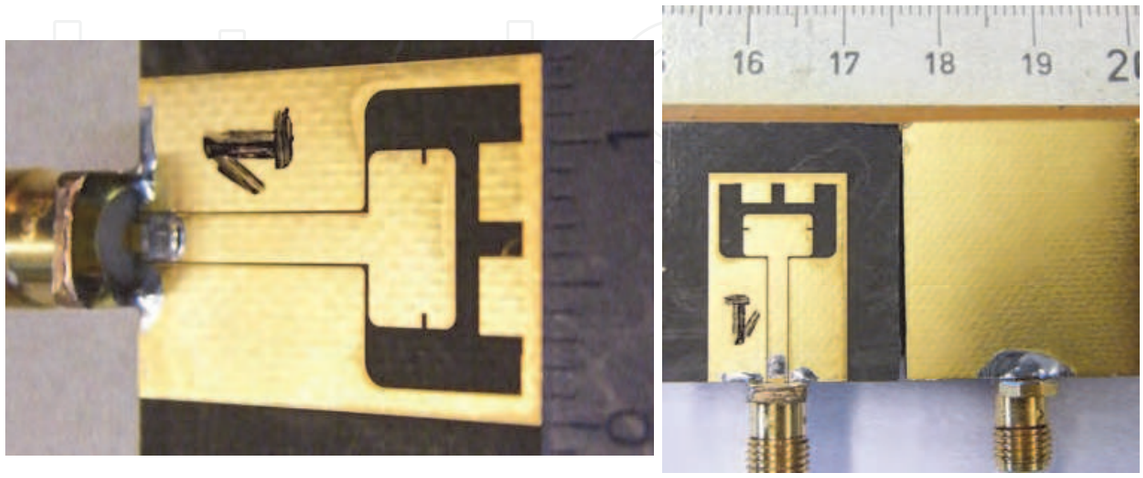

Fig. 10. Prototype with TAB-SMA connector. b) Front and back, dimensions in mm

The optimized design discussed in Section 3 was designed and based on CPWG topology and to be realized in PCB technology. In an initial phase, the optimum physical implementation replicated the configuration resulting from the optimization process (see table 2). However, for feeding the antenna in practice, a sub-miniature SMA connector was used. We experienced that (Tanyer et al. 2009): 1) the close proximity of the comparatively large connector as well as 2) the alteration of the coplanar waveguide's profile due to the soldering had a detrimental impact on the reflection-coefficient performance and on the radiation patterns. As concerns the radiation patterns, experiments (Tanyer, ibid.) have shown strong perturbations due to the diffraction and the scattering from the standard SMA connector, which had dimensions that were comparable with the antenna itself. To counteract these adverse features, the coplanar-waveguide line was extended by an additional 10mm-long section. This resulted in a twofold beneficial effects: i) making it possible to perform a time-domain de-embedding in the reflection coefficient measurements, and ii) creating the possibility to cover the SMA connector with an absorber during the pattern measurements, without affecting the antenna itself. The total coplanar waveguide length then became LF = 13 +10 =23 mm. This choice was made by assuming that the additional transmission line did not result in a noticeable increase in the feed-line losses (Tran et al., 2011), while allowing the feeding section to be covered by absorbing material during the radiation-pattern measurements. Eccosorb HR (from Emerson & Cuming microwave products) was used for this purpose. From the data sheet, the maximum reflectivity of the material was -20 dB.

The proposed DUWB radiator is a quasi-EM antenna, its topology and architecture are created on a *planar-basis* (the base plane *B* defined in section 2.2) with mutual impedance balanced between the quasi-E and the quasi-M counterpart. Now by attaching the SMA to it, the SMA's flange (which is perpendicular to *B*) will immediately disturb the E-M balance of the radiator, because the flange of the SMA-connector acts as an erected reflecting plane which reflects the field of the magnetic part of the quasi-em radiator. The practical prototype of the proposed quasi-EM DUWB has been redesigned, where the effect of the SMA's flange is also taken into account, as shown in Fig.10a.

6.1 Impedance bandwidth simulation and measurement results

To include the disturb contribution of the SMA-connector and the elongation of the CPWG-feed, the prototype are re-optimized and modified as shown by the photograph in Fig.10a. Front ground plane (ring) and back ground plane is made equi-potential via the SMA common-ground as shown by photograph in fig.10b.

Fig.11a compared the calculated and the measured results of the reflection coefficients in full-spectrum of our equipment's capability, good agreement between the calculated and measured result is obtained.

Inspection of the zoom-in plot (Fig. 11b) we see that the prototype measured result covered an impedance bandwidth larger than 100 percent, to our knowledge this is the widest impedance bandwidth ever recorded for a planar, single layer, unidirectional broadside microstrip patch antenna, further more the structure also possessed several usable spectra with deep match at Ka and Q-band.

The measured results have, as a proof-of-concept, demonstrated the feasibility of the introduced concept and technique for bandwidth enhancement as well as controlling other EM-characteristics of the radiator. Nevertheless, the investigation of the proposed prototype

is by no means exhausted the potential of this radiator, inspection of figure 11.a, we anticipate that by careful design and re-optimization of the architecture it is possible to have a unidirectional UWB broadside antenna which could match more closely to the frequency independent impedance bandwidth as predicted 65 years ago by Babinet-Booker formula (Eq.4).

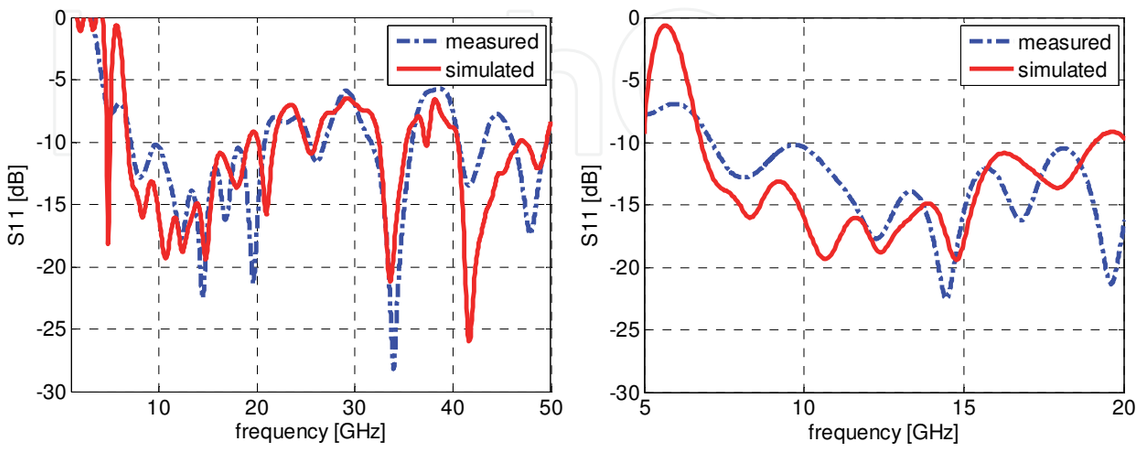

Fig. 11. a) S11 computed vs. measured in full spectrum, b) S11: complete X and Ku coverage

6.2 Farfield measurement set up

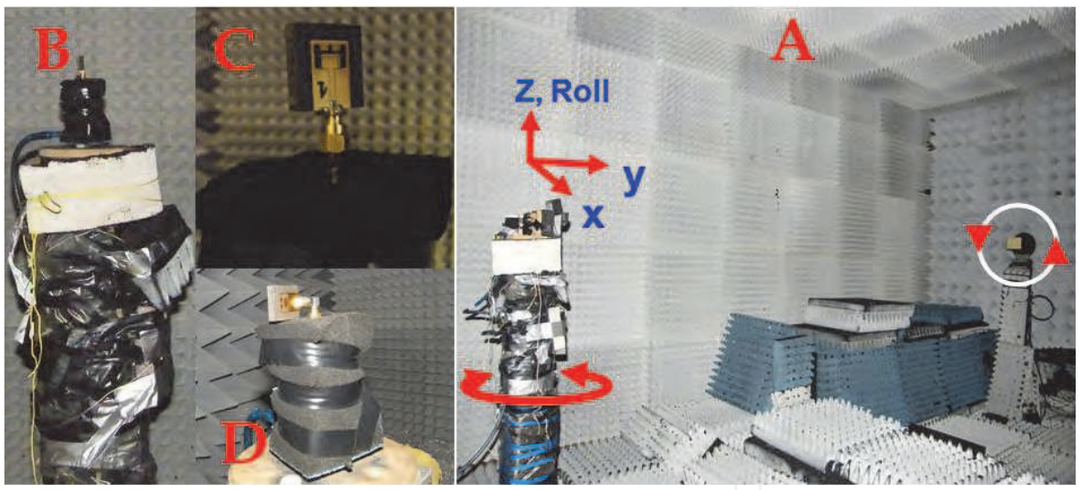

Fig. 12. Patterns measurement set up: a) anechoic chamber DUCAT, b) AUT on the rotatable column, c) Vertical configuration and, d) Horizontal configuration.

Anechoic chamber:
the far field radiation patterns are measured in the Delft University Chamber for Antenna Test (DUCAT); the anechoic chamber DUCAT (Fig.12a) is fully screened, its walls, floor and ceiling are shielded with quality copper plate of 0.4 mm thick. All these aimed to create a Faraday cage of internal dimension of 6 x 3.5 x 3.5 m^3, which will prevent any external signal from entering the chamber and interfering with the measurements. The shielding of the chamber is for frequencies above 2 GHz up to 18 GHz at least 120 dB all around

(Ligthart, 2006). All sides are covered with Pressey PFT-18 and PFT-6 absorbers for the small walls and long walls, respectively. It is found that one side reflects less than -36 dB. All these measures were taken together in order to provide sufficient shielding from other radiation coming from high power marine radars in the nearby areas.

TX:

Single polarization standard horn is used as transmitter (Fig.12a), which can rotate in yaw-y-direction to provide V, H polarizations and all possible slant polarizations. The choice of the single polarization horn above the dual polarization one as calibrator is two-folds: 1) keeps the unwanted cross-polarization to the lowest possible level, 2) and also voids the phase center interference and keeps the phase center deviation to the lowest level.

RX:

Prototype is put as antenna under test (AUT) on the roll-z-rotatable column (Fig.12b). For the measurements of polarimetric components (VV, HV, VH, HH, the first letter denotes transmission's polarization state, the second is for the reception).

Calibration:

The HF-ranges of the Sucoflex-cable, T-adapters and connectors used in this measurement set up all catalogued as 18GHz max, owing to this limitation, we calibrated the PNA with Agilent N4691B cal-kit (1-26GHz).

Configuration setup:

*T*wo measurement setups are configured: i) the vertical reception setup (VRS, Fig.12c) for the receptions of co and cross polarization patterns VV and VH, respectively; ii) the horizontal reception setup (HRS, Fig.12d) for co and cross polarization patterns HH and HV, respectively. Combination of the two spatial reception states (VRS and HRS) with the two polarization states (V,H) is sufficient in providing full polarimetric characterization for the DUT.

6.3 Co-polar radiation patterns (VV) measured with VRS-configuration set-up

The co-polar pattern measurements are carried in the anechoic-chamber DUCAT, Full calibrated spectrum is plotted in Fig.13, typical zoom-in spectra are plotted in Fig.14.

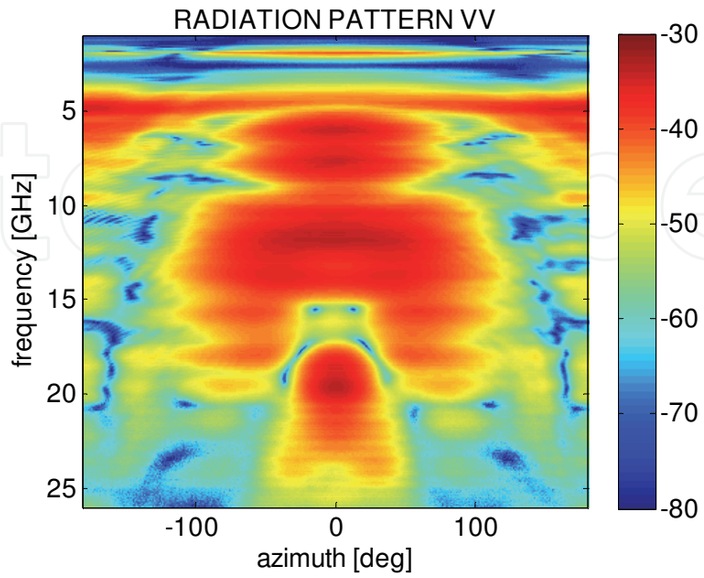

Fig. 13. Measured results: full spectrum Co-polar (VV) radiation patterns

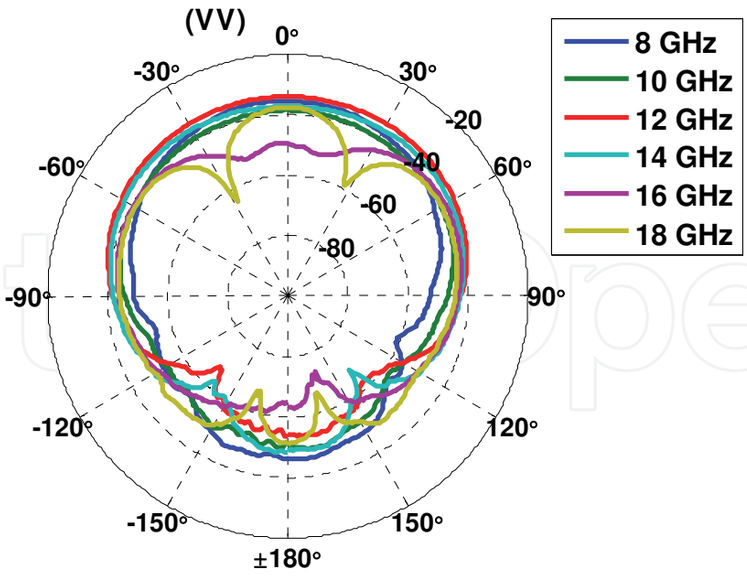

Fig. 14. in-band spectra: stable, symmetrical and repeatable co-polar (VV) uni-directional radiation patterns

As show in both plots, the measured in-band co-polar radiation patterns pertain a perfect symmetry and repeatable in the designated spectrum, this suggests the wideband utilization of this antenna (a UWB antenna is usable if and only if both of its impedance bandwidth and patterns are usable).

6.4 Cross polar radiation patterns (HV) measured with VRS-configuration set-up

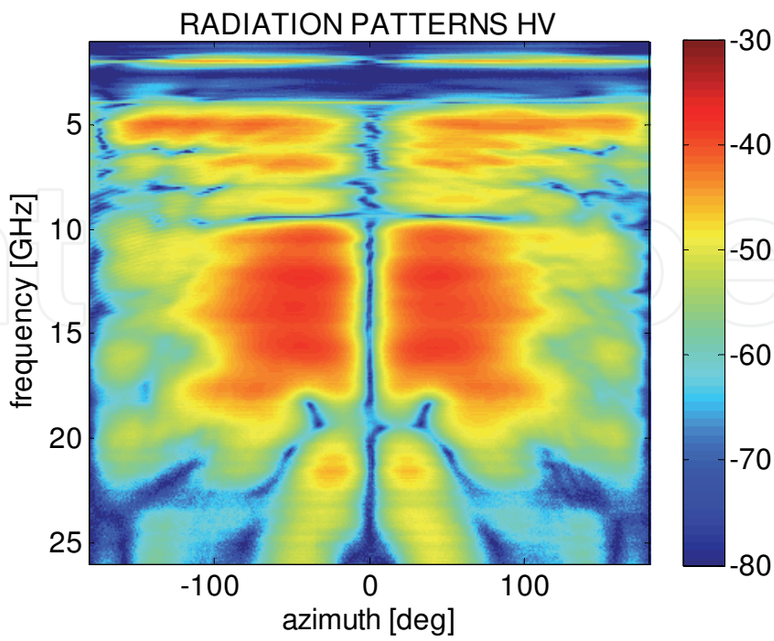

Fig. 15. Measured results: full spectrum Co-polar (HV) radiation patterns

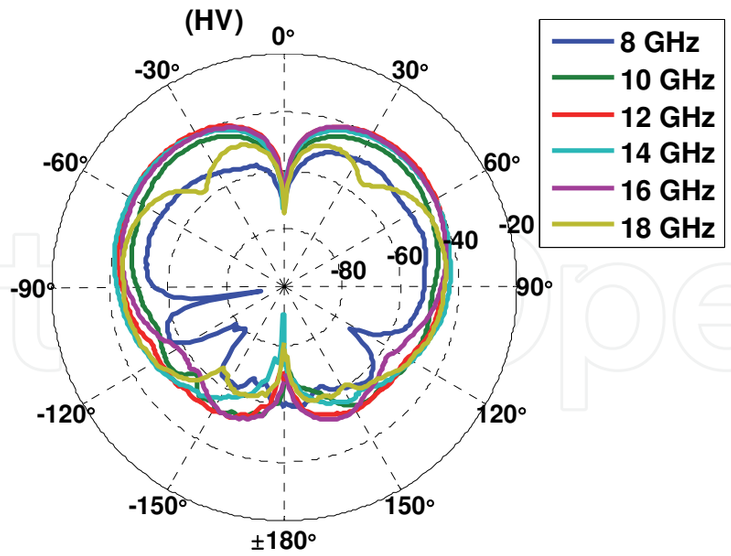

Fig. 16. in-band spectra: stable, symmetrical and repeatable Butterfly–shape of cx-polar(HV) patterns.

The cross-polar patterns measured with VRS configuration. Full spectrum results are plotted in Fig.15, typical zoom-in spectra are plotted in Fig.16. Typical symmetrical butterfly shape of cross polar patterns with exact deep centre as low as -75 dB are measured.

6.5 Co and cross polarization patterns measured with HRS-configuration set-up

For the HRS configuration, the co-polar and cross-polar patterns are measured and plotted in Fig.17a and 17b, respectively. The symmetry is lost in this HRS configuration (Fig.12d) due to the connector, the radiator's ground plane and the mounting column's back-cable (Fig.12b). Nevertheless, the measured patterns are repeatable, and usable as shown.

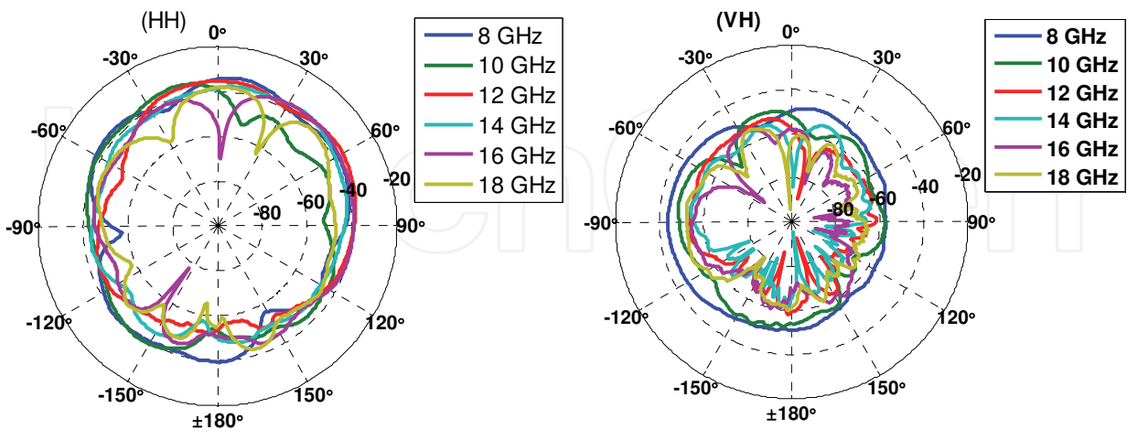

Fig. 17. in-band radiation patterns, a) Co-polar (HH) patterns, b) Cx-patterns (HV)

6.6 In-band co- and cross-polar radiation patterns discussions

The measures co-polar and the cross-polar plotted of the VRS are plotted in rectangular coordinated (Fig.18a &b), which reveal more excellent details which are not observable in

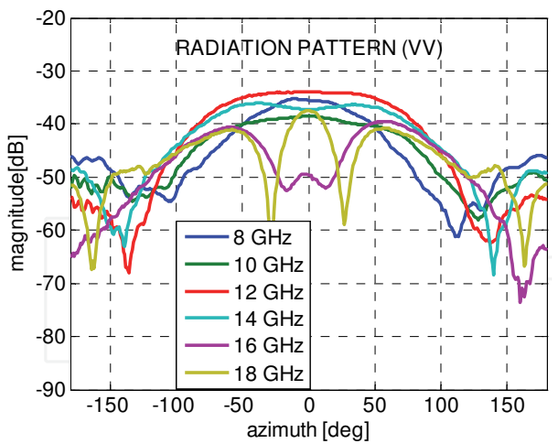

Fig. 18. Constant gain, non-squint co-polar pattern in designed band, VV-case

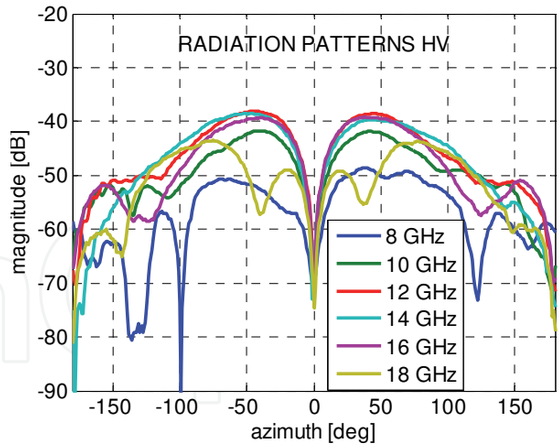

Constant, extremely low cx-polarization (HV) in the designed band

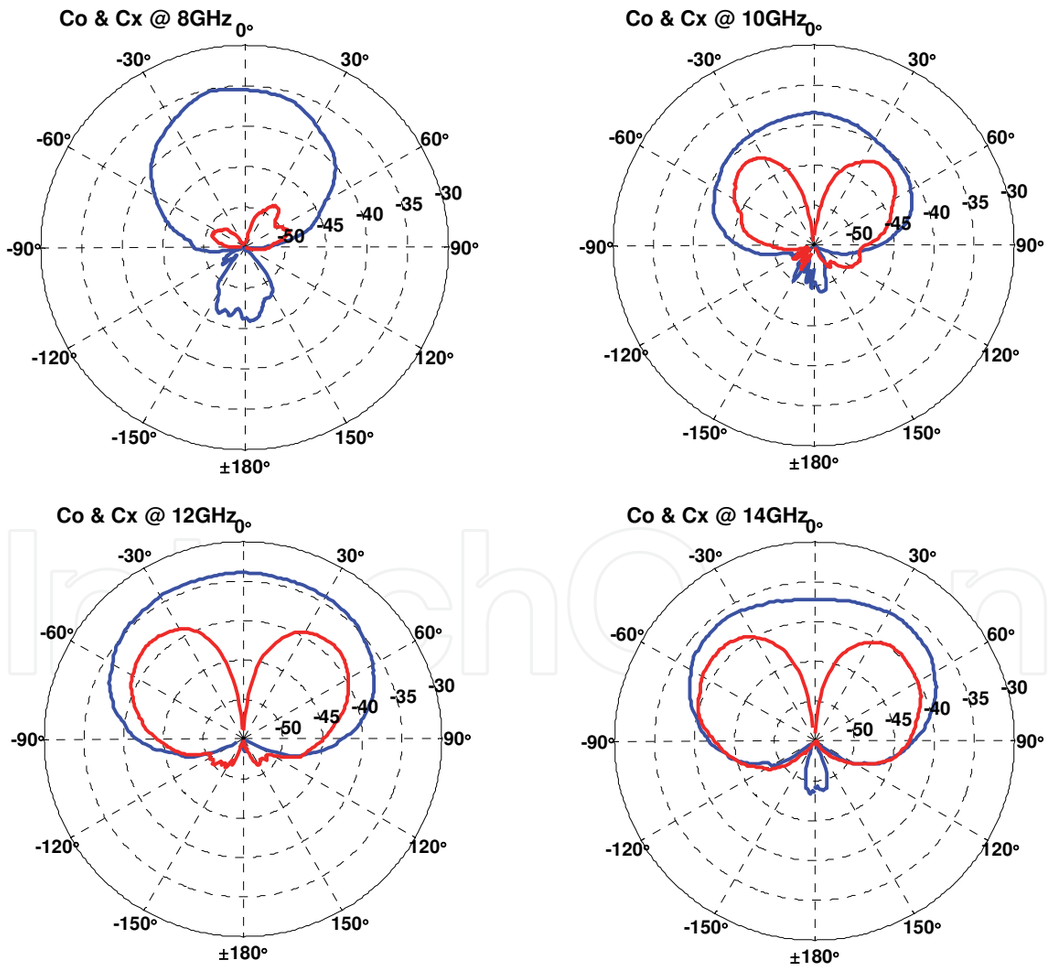

Fig. 19. Typical zoom-in Co-polar (VV) and cx-polar (HV) radiation patterns in the designed band

polar coordinated. This plots displayed: 1) repeatable patterns, 2) minimum front-to-back ratio in all case is >16dB , this value is remarkable for this small size antenna, 3) the patterns come closely to the ideal Silver's theoretical radiator, which guaranties having effectively coverage over the upper hemisphere. 4) the cross-polarization patterns were perfectly symmetric and all have an extremely deep about -75db exactly pointed at broadside of the radiator, this distinct property is possibly the most important requirement for all applications which require extremely high sensitive, accurate sensing and truly 4D space-time information of scatterers, (distance, angle , height, DOA and Doppler).
The measured in-band radiation patterns for 8, 10, 12, 14 GHZ are plotted in Fig.19 a, b, c and d, respectively. The data plotted were raw-power data which are intentionally not normalized. Inspection of the plots, we learn following distinct features of the proposed prototype:

- The radiator is undoubtedly a broadside unidirectional radiator.
- The gain is stable and constant over the designated band.
- The patterns are stable and come very close to the ideal Silver's $\cos \theta^n$ which is very difficult realized in practice.
- The radiator has practically negligible back-lobes, the plots realistically showed very high front to back ratio (FBR), remarkably at 12GHz (where no back-lobe is observed) the FBR at this frequency interpreted a surreal high FBR number, however, it is de facto true measured results.
- The cross-polarization patterns were also very low and exhibit a clear deepest patterns exactly at the pointing direction of the co-polar pattern, this indicated that the polarization purity of this radiator is extremely high, again with number close-to 40dB of cross-polar discrimination (XPD) realized with patch antenna, and in such a UWB bandwidth, is quite unique and unparalleled results. This remarkable property proved that the radiator is very suitable for applications which require extremely high accuracy in sensing, screening or ranging.
- The non-quint radiation patterns over and UWB bandwidth indicated that this prototype will provide accurate bearing resolution and DOA in both short range and long range radar applications.

6.7 Time domain measurements

Fig. 20 shows time-domain setup for measurement and evaluation of: 1) pulse deformation, 2) the semi-omni-radiation characteristics of the AUT. The same prototype is used for TX (left) and RX (right), they both stood on a horizontal foam bar which situated 1.20m above the floor.

6.7.1 Pulse transmission measurements in time domain

Pulse spreading and deformation: Fig.21 showed the time-synchronization between the measured receive pulses (MRP) at three representative angles, qualitative inspection showed that the synchronization-timing the received pulses is very good, there is no pulse spreading took place, these measured features proved that the device is suitable for accurate ranging/ sensing-applications, the small deviation at the beginning of the received pulse is due to RF-leakage (Agilent, AN1287-12, p.38), and at the end of the received pulse are from environments and late-time returns (Agilent, ibid., p.38), Note that the measurements are carried out in true EM-polluted environment as shows in Fig.20, and no gating applied.

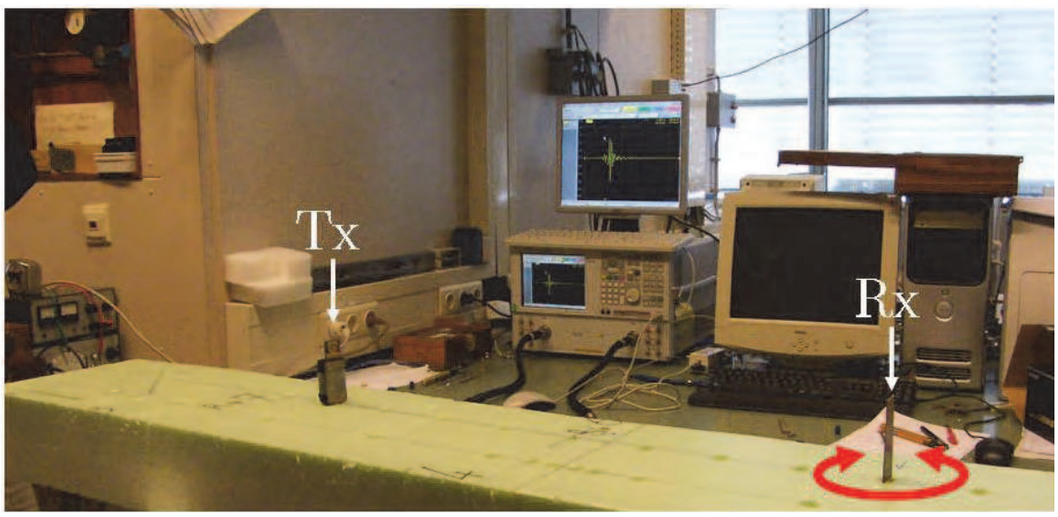

Fig. 20. Time domain measurement setups for co-polar (VV); equipment: Agilent VNA, E8364B; Calibration kit: Agilent N4691B, calibrated method: 2-port 3.5 mm, TRL (SOLT), 300 KHz – 26 GHz.

Uni-directional radiation characteristics: to correctly evaluate the directional property of the AUT, both quantitative characteristics (spatial) and qualitative characteristics (temporal) are carried out, the spatial-properties of prototype are already tested and evaluated in frequency-domain (depicted in Fig.12), and only the temporal-characteristic is left to be evaluated. To evaluated temporal-radiation characteristics, three principal cuts are sufficiently represent the temporal-radiation characteristics of the AUT in the time domain. Due to the editorial limitation, we report here only the most representative case (uni-directional in the azimuthal plane, i.e. co-polar VRS, which represents the most of all realistic reception scenarios, as shown in Fig.20). Fig.21 shows three MRPs of the measurement configuration pictured in Fig.20 with RX 0^0, 45^0, and 90^0 rotated. The results show a perfectly identical in timing, there is no time–deviation or spreading detected between the three cases. Furthermore, although the radiator is planar and unidirectional, it still exhibits a remarkable azimuthal independent property of 3D-symmetric radiators (for the 90^0 configuration, the projection of the receiving aperture vanished, however the prototype still able to receive 60% power as compare to the face-to-face case), this TD-measure results pertained the cos θ-directional property of the radiator, and this is also in agreement with, and as well consolidate the validity of the measured results carried out in the FD-measurement setup.

6.7.2 Transmission dispersion characterization

To evaluate the amplitude spectral dispersion of the prototype, the measured time-domain transmission scattering coefficients of the three co-polar configurations (0^0, 45^0, and 90^0 configurations displayed in Fig.21) were Fourier-transformed in to frequency domain. The measured magnitudes are plotted in Fig.22a, the measured results show a smooth and flat amplitude distribution in the designated band, and all are lower than -42dBm.

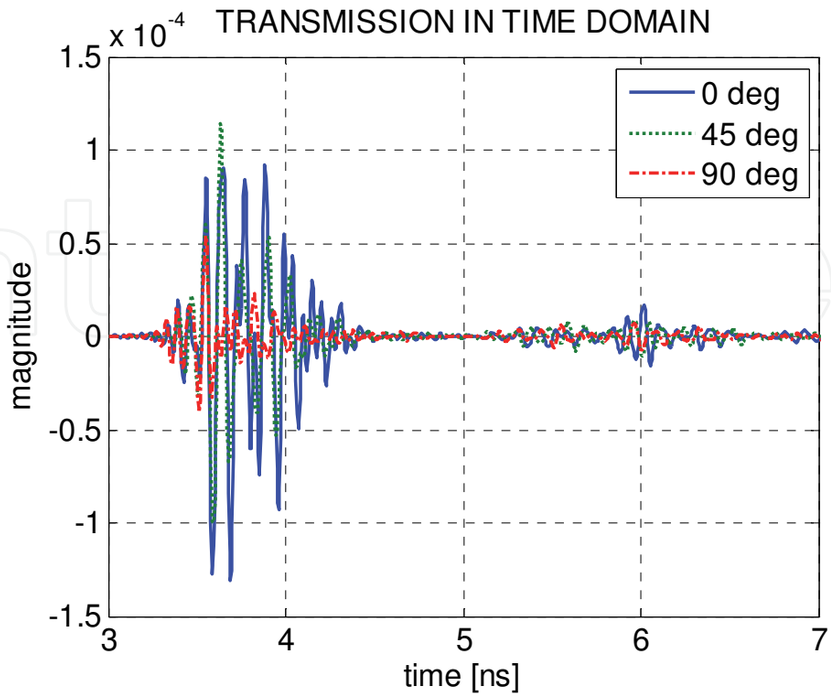

Fig. 21. Time domain measurement setups, equipment: Agilent VNA E8364B; Calibration kit: Agilent N4691B, calibrated method: 2-port 3.5 mm, TRL (SOLT)

6.7.3 Transmission phase delay and group delay

Group-delay is an important gauge by which the highest sensitivity/accuracy of sensors are judged, particularly for sensors/systems which implements phase referencing mode/coherent detection for applications in space geodesy, absolute astronomy (Petrov et al., 2010) and in sensors with independent beam steering for multiple beam applications (Yaron et al., 2010). Low group delay is critical for quint-free operations of the beam-former, preventing lost of tracking and miss-hit, etc.

The measured phase responses of the transmission parameter S_{21} for the three co-polar configurations are plotted in Fig. 22. In narrowband technology, the metric for judging the quality of transmission is the phase-delay, define as $\tau_P = -\theta/\omega$, which is the phase delay between the input and output signals of the system at a given frequency. In wideband technology, however, group delay is a more precise and useful measure of phase linearity of the phase response (Chen, 2007). The transmission group delays for the three above-mentioned configurations are plotted in Fig. 22c. The plots show a flat, stable and negligible variation in group delays in order of sub-nanosecond. The group delays in broadside direction, representative here with RX 0^0, 45^0 rotated, shown almost *identical group delays* (this guaranties for quint-free wide-scan operations of the designate band; this is no surprise because the phase responses of the prototype are almost linear (Fig.22b), thus the group delay, which is defined as the slope of the phase with respect to frequency $\tau_G = -d\theta/d\omega$, resulted accordingly. Note: although the group delay (Fig.22c) is mathematically defined as

a constituent directly related to the phase, but it was impossible to visually observe directly from the phase plot (Fig.22a), but well from the magnitude plot (Fig.22a).

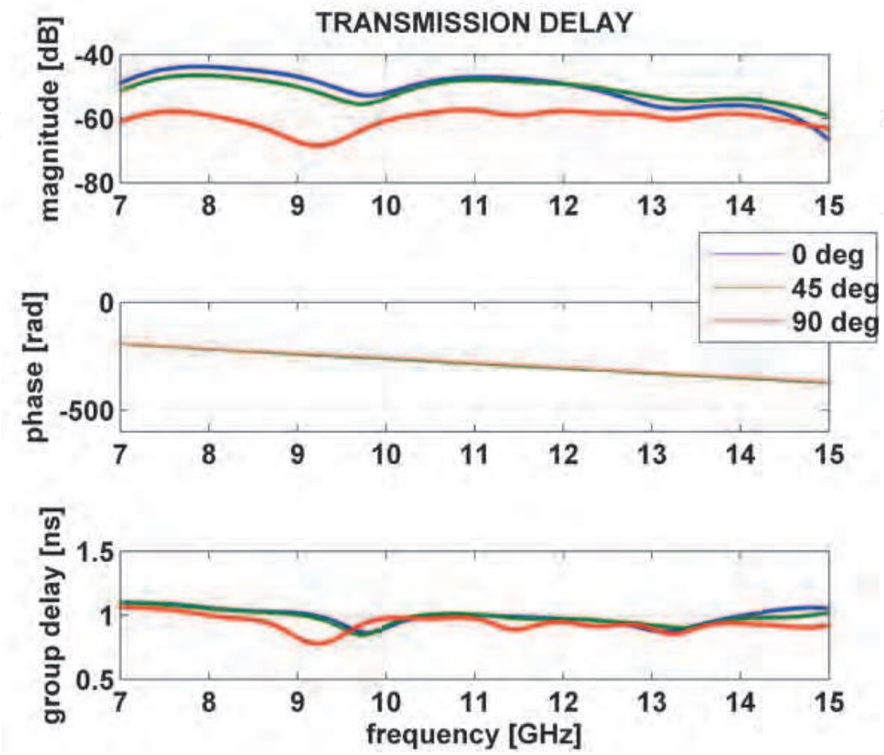

Fig. 22. Transmission dispersion characterization: a) Transmission magnitude, b) Transmission phase, c) Transmission group delay.

7. Acknowledgement

The research reported in this work was effectuated with in the frame of the "Wise Band Sparse Element Array Antennas" WiSE-project, a scientific undergone financed by the Dutch Technology Foundation (Stichting Technische Wetenschapen – STW). This support is hereby gratefully acknowledged. This technological-transfer is made possible to the "Sensor Technology Applied in Reconfigurable Systems for Sustainable Security" STARS-project thanks to the successful collaboration between two national institutions IRCTR (Netherlands), and METRA (Romania), with Thales, TNO, ASTRON and ESA as technological supervisory bodies.

8. Conclusions

In this chapter the top side antennas dilemma and impasses are addressed, the logical solution to this problem is the shift from phased array to active electronic scanned array, key aspects relating to this shift are discussed; the state of the art, trends and activities on wideband-multiband-multifunction AESA is summarized; existing radiators and methods

as well as techniques for creating wideband and unidirectional radiators are convened and reviewed; their advantages and disadvantages are discussed and summarized.

The logical shift in phased array technology to multiband multifunction active electronic scanned array put stringent demands on the applicable radiator. The AESA-applicability implies that the radiator must be unidirectional, small size in array plane and compact in volume. The AESA functional performance required that the radiator must be wideband, linear phase, negligible group delay, low cross polar patterns, accurate pattern heading, stable phase center in the whole covering band.

To comply with these stringent demands, a novel quasi electric-magnetic ultra wideband is proposed; it is designed to comprise all the merits and to eliminate all the demerits of the MPA, SMPA and UWB antennas. The proposed DUWB pertains the linear phase, compactness, low cross-polarization of the MPA, possesses the directional property of the MPA and the SMPA, and has as ultra wideband as common UWB antennas. The prosed antenna's topological structure is simple and its architecture is easy to realize with low cost PCB technology.

Concepts and ideas

Our intent message is not the performances of the proposed prototype but heavily weights on the concepts, the design methodology, and the process of identification of the critical design parameters which are the objectives that we report in this chapter.

- The ideal electric antenna, magnetic antenna are wholly revisited, and the electric-magnetic antenna is corollary added for completeness.
- The concept of quasi electric, quasi magnetic are revisited, and their propositional concept of quasi electric-magnetic antenna is extended to complete the set.
- The main driven idea led to the design of this DUWB radiator is anticipated from the self-complementary principle stated by Babinet-Booker's principle.
- The Babinet-Booker's frequency-independent impedance relation, together with the Mushiake's optimum impedance, are ultimately and functionally applied to the design of the proposed DUWB radiator.
- Distinct concepts and definitions scattered in literature are collected, defused, arranged and systematically and correctly applied to antenna design.
- The concepts 1-4 above led to the quest for a specific topology and architecture that supports the self-complementary principle and hence the frequency-independent (wideband) property.

Methodologies and implementations

- Topology: the CPWG has been chosen for the realization of comprised quasi electric–magnetic radiator.
- Architecture: By forcing the overall dimension of the radiator fixed, the created topology and architecture kept the impedances of the magnetic and electric parts mutual related in accordance with the Babinet-Booker impedance relation. The current-driven quasi-magnetic radiator is formed by the top grounded-ring (i.e circumscribing the quasi-electric radiator also by this ring). By this doing the voltage-driven quasi-electric radiator is automatically embedded inside its complementary counter-part.
- Engineering: several design parameters are created to control the quasi electric-magnetic properties of the proposed radiator, the effects of these design parameters are characterized and analyzed.

- Parameter identification and optimization: Since the E- and M-radiator are imbedded in the same architectural radiator. We observed that any parameter varying of electric (or magnetic) will automatically effectuate it complementary magnetic (or electric) part, so the process of optimization can be reduced by optimization (sweeping) the critical design parameter in identified priority order. We identified the critical design parameters and report their priority herewith: the patch length P3, the patch width P4, the inners tubs P16, the outer stubs P15, the notch length P10, the carves P9; The investigation of other parameters is by no means exhausted, they have their own meaning and functionalities in fine-tuning the performance of the quasi-em radiator, however they effectuated only marginally as compare to the critical ones previously listed and discussed.
- Although the prototype comprised a simplest structure and shape, however superior UWB impedance bandwidth is achieved and stable UWB-patterns are uniquely preserved. This structure, although, can be modified to obtain huge frequency bandwidth, but cannot be one-size-fit-all for gain-size requirement. However, the architecture is flexible enough for scaling up/down its dimensions to match customer's gain-size requirements and applications.

Results

As a proof of concept, a quasi electric-magnetic, planar, unidirectional, broadside UWB prototype is designed, fabricated. Performance of the prototype are tested and evaluated. Good agreements between numerical predictions and measurements are obtained, we reported and demonstrated herby with following results:

- A DUWB radiator comprises all the goods but avoids the bads of the MPAs, SMPAs and the UWBAs has been realized
- The first unidirectional broadside radiator effectively comprised both electric and it complementary part in one *planar* structure, and functionally and partly proved the frequency-independent property stated by Babinet, Booker and Mushiake.
- Minaturization: single dielectric layer, compact with voluminous dimension: 13.4 x 13.4 x 5.537 mm^3. With this size the radiator is small enough for X-phased array applications; no grating lobe will theoretically appear for scanning up to 60° for the whole X-band.
- The "bandwidth and antenna size are inversely related" has been ultimately optimized, the advocated antenna is possibly the one which posses the largest "form factor" to date (BDR: BW(100%)-over-Dimension(13x13mm^2) Ratio)
- UWB: A planar low-profiles (5mm), non-floating ground radiator with performance of over 100% percent bandwidth ever designed, for full coverage of the designated X & Ku band , this being the widest ever obtained with single substrate MPA and perhaps, the widest ever published for a unidirectional broadside patch radiator.
- The prototype possessed all properties required for wide multiband multifunction AESA applications such as: unidirectional, wideband, balanced and flat complex reflection power spectrum, high efficiency, non-squint heading, phase linearity, low dispersion (negligible group delay), polarization purity, low cross polarization, stable phase center, compact and finally the planar and broadside topology make the proposed radiator very attractive for technological-tile which is a critical requirement for dense implementation and integration of radiator with T/R module together with the associated controls and calibrated circuitries.

- Pattern stability: Repeatable patterns in full X-band spectrum, nearly perfectly omni-directional pattern in the "array-plane" (X0Y),
- Time dispersive characteristics: Pulse measurement show excellent pulses synchronization, repeatable pulse patterns, non-squint, constant power over wide angle and fidelity is greater than 90% in the upper hemisphere.
- Parameter sequential order and sweeping methodology are elaborated in details, the priority and role of separable parameters are identified (table.1), and so, instead of multivariable-optimization, the optimization process can be accelerated by carry out sequence of parameter sweeping. The proposed design, optimization procedure can possibly be used as a gauging-process for designing or optimizing similar DUWB structures.
- The proposal antenna could possible be a solution for reducing/resolving the top side antennas problem and to somewhat degree will certainly be a push forwards the network the Network Concentric Operations (NCO)
- The DUWB-prototype has been designed years ago but not published elsewhere; due to editorial limits, we exclusively report here only the design methodology and conceptual approach; detailed mathematical formulation and numerical aspects related to this DUWB prototype will be published in another occurrence.

8. References

Agilent technologies (2007). Time Domain Analysis Using a Network Analyzer, Application Note 1287-12, 2007.

Balanis, C. A. (2005). Antenna theory analysis and design, Wiley & Sons 3rd, New York.

Baum, C.E. (2005), Compact Electric Antenna, Sensor and Simulation Notes, N500.

Booker, H.G. (1946). Slot Aerials and Their Relation to Complementary Wire Aerials, Proc. IEE, pt. IIIA, no. 4, pp. 620-629, April 1946.

Brown, D., Fiscus, T. E, Meierbachtol, C. J (1980). Results of a study using RT 5880 material for a missile radome, In: *Symposium on Electromagnetic Windows*, 15th, Atlanta, GA, June 18-20, Proceeding (A82-2645, 11-32), Georgia Institute of Technology, p.7-12.

Chen, Z. N. And Quing, X,(2005) Research and development of plannar UWB antennas. *Proceeding of the APMC 2005*.

Chen Z.N. (2007). Antenna Elements for Impulse Radio, In: *Ultra-wideband Antennas and Propagation for Communications, Radar and Imaging*, Allen B. (Ed.),Wiley & Sons.

Elek, F. et al. (2005), A uni-directinal ring slot antenna achieved by using Electromagnetic bandgap surface. *IEEE Trans. on AP.*, vol. 53, no. 1, Jan. 2005, pp. 181-190.

FCC (2002). Federal Communications Commission, FCC 02-48, ET-Docket 98-153, "*First Report and Order*", Apr. 2002.

FCC (2004), Federal Communications Commission, FCC 04-285, ET-Docket 98-153, "*Second Report and Order and Second Memorandum Opinion and Order*", Dec. 2004.

Hecht, E.,(2001), Optics, 4th edition, Addison Wesley,Aug, 2001.

Huang, Y. & Boyle, K. (2008). *Antennas from Theory to Practice*, John Willey and Sons, Singapore, 2008, pp.64.

IEEE Std 145-1983 (1983). *IEEE Standard Definitions of Terms for Antennas*, New York, IEEE Press, 1983, pp.11-16.

Karoui, M. S., Ghariani, H., Samet, M., Ramadi, M., Pedriau, R. (2010). Bandwidth Enhancement of the Square Rectangular Patch Antenna for Biotelemetry applications, *International journal of information systems and telecommunication engineering,* v.1, 2010, iss.1, pp.12-18.

Kshetrimayum, R. S., Pillalamarri, R. (2008). Novel UWB printed monopole antenna with triangular tapered feed lines, *IEICE Electronics express*, vol.5, No. 8, pp. 242-247.

Lamanna, M and Huizing, A. G.(2006), Scalable multifunction active phased array systems: from concept to implementation, *IEEE Int. Radar Conference, Verona, NY, Apr. 2006.*

Lee, F.L. & Luk, K.M (2011), Microstrip patch antennas, Imperial College Press, ICP ltd., London, 2011.

Ligthart, LP (2006). Antennas and propagation measurement techniques for UWB radio, *Wireless personal communications*, 37(3-4), pp.329-360.

Mushiake, Y.(1996), Self-Complementary Antennas: Principle of Self-Complementarity for Constant Impedance, Springer Verlag, London, 1996.

Petrov, L., Phillips, C., Bertarini, A., Murphy, T. and Sadler, E.M.,(2010). "The LBA Calibrator Survey of southern compact extragalactic radio sources — LCS1", Mon. Not. of Roy. Astron. Soc.,000,pp.1-13, Dec. 2010.

Rahayu, H., Rahman, T. A., Ngah, R., Hall, P. S. (2008). Slotted ultra wideband antenna for bandwidth enhancement, 2008, *Loughborough A&P Conference*, Loughborough, UK.

Rahim, M. K. A. & Gardner, P. (2004). The design of nine element quasi microstrip log periodic antenna, MW&RF *conference*, RFM 2004,Selangor, Malaysia, pp.132–135.

Rao Q. & Denidni T. A. (2007), Ultra-Wideband and Uni-Directional Radiation Slot Antenna for Multi-Band Wireless Communication Applications, Wireless Personal Communications v. 41, pp. 507–516, 2007.

Rmili, H. & Floc'h, J. M. (2008). Design and analysis of wideband double-sided printed spiral dipole antenna with capacitive coupling, *Microwave and optical technology letters,* Vol. 50, No.5, pp. 312-1317.

Schantz, H.G. and Bames, M., (2001),"The COTAB UWB Magnetic Slot Antenna," IEEE International Symposium on Antennas and Propagation Digest, 4, 2001, pp.104-107.

Schantz, H. G and Barnes, M. (2003). UWB magnetic antenna, *IEEE International Symposium on Antennas and Propagation Digest*, 3, 2003, pp.604-607.

Schantz, H. G. (2004). A brief history of UWB antennas, *IEEE Aerospace and Electronic Systems Magazine*, vol .19(4), pp.22-26, 2004.

Schantz, H, (2005); The Art and Science of Ultra-Wideband Antennas, Artech House Publishers Boston, MA, July, 2005.

Simons, R. N. (2001). *Coplanar Waveguide Circuits, Components, and Systems*, John Wiley & Sons, New York, 2001.

Stutzman, W.L. and Thiele, G.A.(1997), Antenna theory and design, Wiley & Sons, 1887.

Suh, S. S., et al., (2004); A novel printed dual polarized broadband antenna, the fourclover antenna; *Proceeding of the international symposyum on antenna and Progation, ISAP 2004,Sendai, Japan,* pp. 77-80.

Tanyer, F. M, Tran, D., Lager, I. E., Ligthart, L. P. (2009a). CPW-fed Quasi–Magnetic Printed Antenna for Ultra-Wideband Application, *IEEE Antennas and Propagation Magazine*, Vol.51, No.2, April 2009, 1, pp.61-70.

Tanyer, F.M; Lager, I. E., Mateos, R. M., Craeye, C(2009b).; Design of an AMC Plane for a Unidirectional, Low-profile Tulip-Loop antenna, Proceeding of the 3rd European Conference on Antennas and Propagation, EuCAP2009, Berlin, Germany.

Tavik, G. C. et al.(2005), The Advance Multifunction RF concept, IEEE Transaction on MTT, Vol.53,No.3, Mar. 2005, pp.1009-1020.

Tayefeh,M., Aligodarz, K., Rashidian, A. (2004), Wideband Miniaturized L-Probe Fed Fractal Clover Leaf Microstrip Patch Antenna, in: *Proceedings of JINA2004,* France, 2004

Tibbitts, B and Baron, N. (1999), Topside design of warships : a 100 year perspective ; Naval Engineers Journal, vol. 111, is. 2, pp. 27–44, Mar. 1999.

Tourette, S., Fortino, N., Kossiavas, G. (2006). Compact UWB printed antennas for low frequency applications matched to different transmission lines, *Microwave and optical technology letters*, Vol. 49, No.6, pp.1282-1287.

Tran, D., Tanyer-Tigrek, F. M., Vorobyov, A., Lager, I.E. & Ligthart, L.P.(2007). A Novel CPW-fed Optimized UWB printed Antenna, In: *Proceedings of the 10th European conference on wireless technology,* p.40-43, Munich, Germany, October 8-10, 2007.

Tran, D., Tanyer, F.M., Lager, I.E, Ligthart, L.P.(2009); A Novel Unidirectional Radiator with Superb UWB Characteristics for X-band Phased Array Applications; 3rd European Conference on Antennas and Propagation,EuCAP2009, Berlin, Germany, Mar. 2009.

Tran, D., Coman, C.I., Tanyer, F.M., Szilagyi, A., Simeoni, M., Lager, I. E., Ligthart, L. P. & van Genderen, P.(2010).The relativity of bandwidth – the pursuit of truly ultra wideband radiators, In: *Antennas for Ubiquitous Radio Services in a Wireless Information Society*, Lager, I. E (Ed.), pp.55-74, IOS Press, 2010, Amsterdam.

van Genderen, P. (2003), The APAR multifunction radar, system overview, Proceeding of the international symposium on Phased Array Systems and Technology, 17 Oct. 2003, pp.241-246, Boston, MA, 2003.

Wikipedia2011 ; http://en.wikipedia.org/wiki/Active_Electronically_Scanned_Array.

Wu, Q and Jin, R. (2010); On the Performance of Printed Dipole Antenna With Novel Composite Corrugated-Reflectors for Low-Profile Ultrawideband Applications; IEEE Trans. on AP. vol. 58, no. 12, dec. 2010, pp.3839-3846.

Wu, X.H, Chen, Z.N. & Chia, M.Y.W,(2003), Note on antenna design in UWB wireless communicaiton systems, IEEE conference on UWB and Technologies,p. 503–07.

Yaron, L., Rotman, R., Zach, S. & Tur, M.(2010), Photoniv beamformer receiver with multiple beam capabilities. IEEE photonic technolgy letters, vol.22, no.23, Dec.2010

Zhang, X., Wu, W., Yan, Z. H., Jiang, J. B. & Song, Y. (2009). Design of CPW-Fed monopole UWB antenna with a novel notched ground, *Microwave and optical technology letters*, Vol. 51, No.1, pp. 88-91.

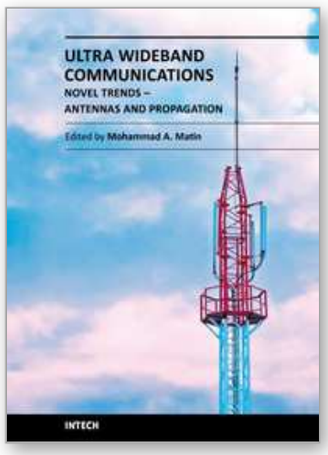

Ultra Wideband Communications: Novel Trends - Antennas and Propagation

Edited by Dr. Mohammad Matin

ISBN 978-953-307-452-8
Hard cover, 384 pages
Publisher InTech
Published online 09, August, 2011
Published in print edition August, 2011

This book explores both the state-of-the-art and the latest achievements in UWB antennas and propagation. It has taken a theoretical and experimental approach to some extent, which is more useful to the reader. The book highlights the unique design issues which put the reader in good pace to be able to understand more advanced research.

How to reference

In order to correctly reference this scholarly work, feel free to copy and paste the following:

D. Tran, N. Haider, P. Aubry, A. Szilagyi, I.E. Lager, A. Yarovoy and L.P. Ligthart (2011). A Novel Directive, Dispersion-Free UWB Radiator with Superb EM-Characteristics for Multiband/Multifunction Radar Applications, Ultra Wideband Communications: Novel Trends - Antennas and Propagation, Dr. Mohammad Matin (Ed.), ISBN: 978-953-307-452-8, InTech, Available from: http://www.intechopen.com/books/ultra-wideband-communications-novel-trends-antennas-and-propagation/a-novel-directive-dispersion-free-uwb-radiator-with-superb-em-characteristics-for-multiband-multifun

INTECH
open science | open minds

InTech Europe
University Campus STeP Ri
Slavka Krautzeka 83/A
51000 Rijeka, Croatia
Phone: +385 (51) 770 447
Fax: +385 (51) 686 166
www.intechopen.com

InTech China
Unit 405, Office Block, Hotel Equatorial Shanghai
No.65, Yan An Road (West), Shanghai, 200040, China
中国上海市延安西路65号上海国际贵都大饭店办公楼405单元
Phone: +86-21-62489820
Fax: +86-21-62489821

IntechOpen